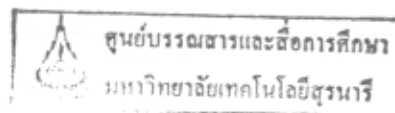


การกระเจิงแบบยืดหยุ่นของโปรตอน-โปรตอนพลังงานสูง
ในแบบจำลองการแลกเปลี่ยนเมซอน

นายเข้ม พุ่มสะอาด



วิทยานิพนธ์นี้เป็นส่วนหนึ่งของการศึกษาตามหลักสูตรปริญญาวิทยาศาสตรมหาบัณฑิต

สาขาวิชาฟิสิกส์

มหาวิทยาลัยเทคโนโลยีสุรนารี

ปีการศึกษา 2543

ISBN 974-7359-61-8

PROTON-PROTON HIGH-ENERGY ELASTIC SCATTERING IN MESON EXCHANGE MODEL

Mr. Kem Pumsa-ard

THE CENTER FOR LIBRARY RESOURCES AND EDUCATIONAL MEDIA
SURANAREE UNIVERSITY OF TECHNOLOGY

**A Thesis Submitted in Partial Fulfillment of the Requirements
for the Degree of Master of Science in Physics**

Suranaree University of Technology

Academic Year 2000

ISBN 974-7359-61-8

Thesis Title

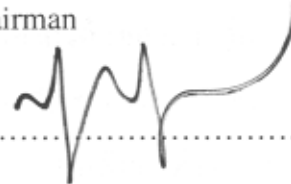
**Proton-Proton High-Energy Elastic Scattering
in Meson Exchange Model**

Suranaree University of Technology Council has approved this thesis
submitted in partial fulfillment of the requirements for a Master's Degree

Thesis Examining Committee



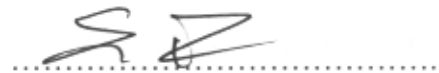
(Assoc. Prof. Dr. Prasart Suebka)
Chairman



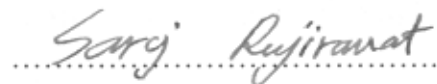
(Dr. Yupeng Yan)
Thesis Advisor



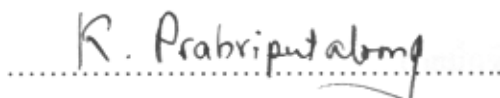
(Prof. Dr. Edouard B. Manoukian)
Member



(Assoc. Prof. Dr. Samnao Phatisena)
Member



(Dr. Saroj Rujirawat)
Member



(Assoc. Prof. Dr. Kasem Prabripataloong)

Vice Rector for Academic Affairs



(Assoc. Prof. Dr. Tassanee Sukosol)

Dean / Institute of Science

เข้ม พุ่มสะอาด : การกระเจิงแบบยืดหยุ่นของโปรตอน-โปรตอนพลังงานสูง
ในแบบจำลองการแลกเปลี่ยนเมซอน (PROTON-PROTON HIGH-ENERGY
ELASTIC SCATTERING IN MESON EXCHANGE MODEL)

อ.ที่ปรึกษา : ดร. ยูเป็ง แขน, 76 หน้า. ISBN 974-7359-61-8

วิทยานิพนธ์นี้เป็นการศึกษาการกระเจิงแบบยืดหยุ่นของโปรตอน-โปรตอนพลังงานสูง ($s=552.3$ จนถึง 3906.3 จิกะอิเล็กตรอนโวลต์²) ในแบบจำลองการแลกเปลี่ยนแบบอนุภาคเดี่ยว ค่าที่ได้จากทางทฤษฎีประกอบขึ้นจากค่าคงตัวของการคู่ควบหลายๆ ค่าโดยผลจากทางทฤษฎีสามารถอธิบายลักษณะเฉพาะที่สำคัญของผลการทดลองอันได้แก่ ค่าความชันที่แตกต่างกันจำนวนสามค่าที่การถ่ายโอนโมเมนตัมค่าต่างๆ และโครงสร้างแบบคิพ (dip-structure) จากการศึกษาพบว่าในการกระเจิงแบบยืดหยุ่นของโปรตอน-โปรตอนพลังงานสูง อันตรกิริยากลุ่มหมอกของควาร์ก-แอนติควาร์ก (quark-antiquark sea) มีบทบาทสำคัญยิ่งกว่าอันตรกิริยากลุ่มหมอกของควาร์ก-กลูออน (quark-gluon) แม้แต่ที่การถ่ายโอนโมเมนตัมสูงๆ นอกจากนี้จากผลการศึกษา เรายังสามารถพิจารณาได้ว่าโปรตอนประกอบขึ้นมาจากสองส่วน อันได้แก่ (1) แกน (core) ซึ่งมีรัศมีน้อยกว่า 0.3 เฟร์มี โดยมีควาร์กจำนวนสามตัวบรรจุอยู่ภายใน และ (2) กลุ่มหมอกของควาร์ก-แอนติควาร์ก ซึ่งกระจายตัวอยู่รอบๆ แกนกลาง สำหรับกลุ่มหมอกของควาร์ก-แอนติควาร์กนั้นมีการกระจายตัวแบบขึ้นอยู่กัอันตรกิริยา โดยมีรัศมีประมาณ 0.7 เฟร์มี สำหรับอันตรกิริยาอย่างแรง (strong interaction) และมีรัศมีประมาณ 0.8 เฟร์มี สำหรับอันตรกิริยาแบบแม่เหล็กไฟฟ้า (electromagnetic interaction)

สาขาวิชาฟิสิกส์

ลายมือชื่อนักศึกษา.....*Kem Pumsaard*.....

ปีการศึกษา 2543

ลายมือชื่ออาจารย์ที่ปรึกษา.....*[Signature]*.....

KEM PUMSA-ARD: PROTON-PROTON HIGH-ENERGY ELASTIC

SCATTERING IN MESON EXCHANGE MODEL:

THESIS ADVISOR: YUPENG YAN, Ph.D. 76 PP. ISBN 974-7359-61-8

The high-energy proton-proton elastic scattering is studied for a large energy region (s from 552.3 to 3906.3 GeV^2) in the one-body-exchange model. By fitting the theory to the experimental data, an estimate is made of the various coupling constants. The main features of the experimental data, the three slopes at different momentum transfer regions and the dip-structure, are well repeated. The study indicates that the quark-antiquark sea interaction is dominant for the high-energy proton-proton elastic scattering over the direct quark-gluon interaction even for high momentum transfers. The proton is an object composed of two components: a core with a size less than 0.3 fm in radius in which three quarks of point-like are confined, and a surrounding quark-antiquark sea. The quark-antiquark sea may present different distributions and hence different sizes for different interactions with a size around 0.7 fm in radius for the strong interaction and a size around 0.8 fm for the electromagnetic interaction.

สาขาวิชาฟิสิกส์

ลายมือชื่อนักศึกษา.....

ปีการศึกษา 2543

ลายมือชื่ออาจารย์ที่ปรึกษา.....

Acknowledgments

First of all, I would like to thank my thesis advisor, Dr. Yupeng Yan, for his kindness, excellent suggestion throughout this work and motivating me to the world of nuclear and particle physics.

I would like to thank Prof.Dr. Edouard B. Manoukian for the helpful discussion about my work, and about modern physics.

I would like to thank the Institute for the Promotion of Teaching Science and Technology.(IPST) for supporting my study related to this thesis.

I would like to thank Mr.Seckson Sukkhasena for setting up the Latex program in my PC and for his advice on the Latex program.

I would like to thank Miss Piyada Jitthungprasert for helping me find articles in the Mahidol Library. She always cheered me up whenever I got problems in the work.

Finally, thanks to my family and to all my friends for all the good things they gave to me.

Kem Pumsa-ard

Contents

	Page
Abstract (Thai).....	I
Abstract (English).....	II
Acknowledgments.....	III
Contents.....	IV
List of Tables.....	VII
List of Figures.....	VIII
Chapter	
I. Introduction.....	1
II. The Meson Exchange Model.....	4
2.1 Nucleon Structure and Nucleon-Nucleon Interaction.....	4
2.2 Meson Exchange in Strong Interaction.....	9
III. Formulation.....	13
3.1 Center of Mass System.....	14
3.2 The Differential Cross Section.....	16
3.3 Lagrangian.....	21
3.3.1 Photon Exchange.....	23
3.3.2 π Meson Exchange.....	26
3.3.3 ρ Meson Exchange.....	27

Contents (Continued)

	Page
3.3.4 ω Meson Exchange.....	28
3.3.5 σ Meson Exchange.....	29
3.3.6 $f_2(1270)$ Meson Exchange.....	29
3.3.7 $\omega(1420)$ Meson Exchange.....	31
IV. Proton-Proton Elastic Scattering in Meson Exchange Model.....	35
4.1 Proton-Proton Scattering with Small Momentum Transfer.....	35
4.2 Proton-Proton Scattering with Large Momentum Transfer.....	44
4.3 Proton Size.....	46
V. Discussion and Conclusion.....	54
5.1 Conclusion.....	54
5.1.1 The Model.....	54
5.1.2 Theoretical Differential Cross Section.....	54
5.1.3 Structure of Proton.....	55
5.2 Comments on the Results.....	55
5.2.1 The $\omega(1420)$ Coupling Constant.....	55
5.2.2 Coulomb-Strong Interference Region.....	56
References.....	57

Contents (Continued)

	Page
Appendices	61
Appendix A. The Mandelstam Variables	62
Appendix B. The Dirac Spinor	64
Appendix C. Differential Cross Section	68
Appendix D. Vertex Functions for $NN\gamma$, $NN\rho$, and NNf_2 Systems	72
D.1 Vertex Function for $NN\gamma$ Coupling.....	72
D.2 Vertex Function for $NN\rho$ Coupling.....	73
D.3 Vertex Function for NNf_2 Coupling.....	74
Biography	76

List of Tables

Table	Page
3.1 Properties of selected mesons.....	22
4.1 The set of parameters best fitted to the experimental data in this work.....	45

List of Figures

Figure		Page
2.1(a)	$d\sigma/dt$ vs. $ t $ at $s = 3906.3 \text{ GeV}^2$ in the small $ t $ region.....	6
2.1(b)	$d\sigma/dt$ vs. $ t $ at $s = 3906.3 \text{ GeV}^2$ in the large $ t $ region.....	7
2.2	Detail structure of nucleon.....	9
3.1(a)	The direct diagram for the proton-proton elastic scattering.....	15
3.1(b)	The cross diagram for the proton-proton elastic scattering.....	15
3.2(a)	The direct process for $1+2 \rightarrow 3+4$ in the CM system.....	17
3.2(b)	The cross process for $1+2 \rightarrow 3+4$ in the CM system.....	17
3.3(a)	$e^-e^-\gamma$ vertex in $e^-+e^- \rightarrow e^-+e^-$	25
3.3(b)	$pp\gamma$ vertex in $p+p \rightarrow p+p$	25
3.3(c)	pp -meson vertex in strong interaction in meson exchange model.....	25
3.4	Contribution of the exchange-particle to the total amplitude.....	34
4.1(a)	$d\sigma/dt$ vs. $ t $ due to γ and $\gamma+\omega$ exchanges for $ t < 0.01 \text{ (GeV/c)}^2$, $s = 552.3 \text{ GeV}^2$	40
4.1(b)	$d\sigma/dt$ vs. $ t $ due to γ and $\gamma+\omega$ exchanges for $ t < 0.1 \text{ (GeV/c)}^2$, $s = 552.3 \text{ GeV}^2$	41
4.1(c)	$d\sigma/dt$ vs. $ t $ due to γ and $\gamma+\omega$ exchanges for $ t < 0.01 \text{ (GeV/c)}^2$, $s = 942.5 \text{ GeV}^2$	42

List of Figures (Continued)

Figure		Page
4.1(d)	<i>dσ/dt</i> vs. $ t $ due to γ and $\gamma+\omega$ exchanges for $ t < 0.1$ (GeV/c) ² , $s = 942.5$ GeV ²	43
4.2(a)	Theoretical prediction for <i>dσ/dt</i> compares to experimental data for $s=552.3$ GeV ²	47
4.2(b)	Theoretical prediction for <i>dσ/dt</i> compares to experimental data for $s=942.5$ GeV ²	48
4.2(c)	Theoretical prediction for <i>dσ/dt</i> compares to experimental data for $s=1998.1$ GeV ²	49
4.2(d)	Theoretical prediction for <i>dσ/dt</i> compares to experimental data for $s=2787.8$ GeV ²	50
4.2(e)	Theoretical prediction for <i>dσ/dt</i> compares to experimental data for $s=3906.3$ GeV ²	51

Chapter I

Introduction

Proton-proton elastic scattering has been studied over forty years, mainly in 1970's. There is a huge number of high-quality experimental data available in the market, but the theoretical understanding of the reaction is very poor. The theoretical study of the nucleon-nucleon scattering is still on the model level, such as geometric model (Serber, 1963; Hansen and Kisch, 1977), meson-exchange model (Landshoff, 1974; Gibbs and Loiseau, 1994) and quark model (Brodsky, Carlson, and Lipkin, 1979; Farrar, Gottlieb, Sivers, and Thomas, 1979). The geometric model is just a semi-classical one, but fits the best the unpolarized differential cross section data of the proton-proton elastic scattering, compared to other models. The quark model, the best candidate of the strong interaction, based on Quantum Chromodynamics (QCD), sounds the best. Unfortunately, however, the quark model yields the poorest explanation of the experimental data. The meson-exchange model lies just between other two models, neither as fundamental as the quark model nor as phenomenological as the geometric model, understands experimental data better than the quark model. For all the models mentioned above, considering only the unpolarized experiments, the most difficult problem is the dip-structure of the proton-proton invariant differential cross section. Up to now, only the geometric model can reproduce this structure in part.

In the present understanding, nucleon is a bound state of three quarks, or say, a “bag”, in which three quarks are confined. Around such a bag there exists a quark-antiquark sea which is usually called meson cloud. The strong interaction between nucleons arises not only from the direct interaction of valence quarks inside nucleons, but also from the sea quark interaction. The sea quark interaction might be “parameterized” to the interaction of meson-exchange. The important question is : How large is the bag within the nucleon? If the bag is large, there will be small space for the quark-antiquark sea, which means that the interaction due to the meson cloud is small. On the other hands, if the bag is small, there will be plenty of space available for the quark-antiquark sea, and the interaction arising from the meson cloud will be prominent. In the MIT bag model (Chodos, Jaffe, Johnson, Thorn, and Weisskopf, 1974) the bag is in the order of 1.0 fm and the meson cloud is treated as a perturbation, which results in that the effect of the meson exchange for the nucleon-nucleon is small. In the little bag model (Brown and Rho, 1979), the bag is about 0.35 fm and the effect of the exchange meson is significant. The cloudy bag model (Thomas and Thèberge, 1981) with the size of the bag about 0.80 fm lies between the MIT bag model and the little bag model.

The concept of meson exchange for the strong interaction was first proposed by Yukawa in 1935. Yukawa’s one-pion-exchange theory was extended to multi-pion-exchange and even heavier mesons soon after the pion was discovered. Various meson exchange models have proposed to describe the strong interaction between nucleons at low and medium energies. The most famous models are the Paris potential described in the work of Cottingham, Locombe, Richard, and Mau (1973) and the Bonn potential as reviewed by Machleidt, Holinde, and Elster

(1987), which are consistent with the low and medium energy nucleon-nucleon reactions. Models in the meson exchange theory are still under improvement and even development for both the low and high energy nucleon-nucleon strong interaction. In the high energy sector, models are developed mainly on the line of multi-boson-exchange, which are usually very complicated.

Our main purpose of this study is to understand the differential cross section of the proton-proton elastic scattering process at the high energy regime in the one-boson-exchange (OBE) theory which is successfully describes the scattering process at low and intermediate energy, and reveals the radii of the three-quark kernel and the meson cloud. In this work, we will treat the nucleon as a composite structure of the quark kernel and the meson cloud described above. The interaction between protons is mainly contributed by the meson cloud interaction (or say, sea-quark interaction) which can be “parameterized” into the meson-exchange.

The outline for this thesis is as following: In Chapter II we give a brief review of the idea of the meson exchange proposed by Yukawa, and also give some general ideas about the present model. The formulation for the proton-proton elastic differential cross section is given in Chapter III, and the theoretical study is presented in Chapter IV. Finally, in Chapter V, deals with conclusions and discussions.

Chapter II

The Meson Exchange Model

In this chapter, we introduce the model of exchanging massive mesons responsible for the strong interaction between nucleons. We shall begin with analyzing the experimental data in high energy scattering process. The experiments in high energy scattering process reveal that there should be two different components which contribute to the size of nucleon. That is the structure of nucleon can be viewed as composed of, the 3-quark core (also called kernel) which has the small radius within nucleon and the meson cloud which surrounds the kernel, extending to some distance. Next, we consider the historical idea of the exchange of mesons in the strong interaction first proposed by Yukawa. The interaction between nucleons will be shortly discussed in the framework of meson-exchange model and also the exchange of a photon in the electromagnetic interaction for the charged-nucleons. Evidences from scattering process pointed to the existence of the meson exchange between nucleons are also discussed.

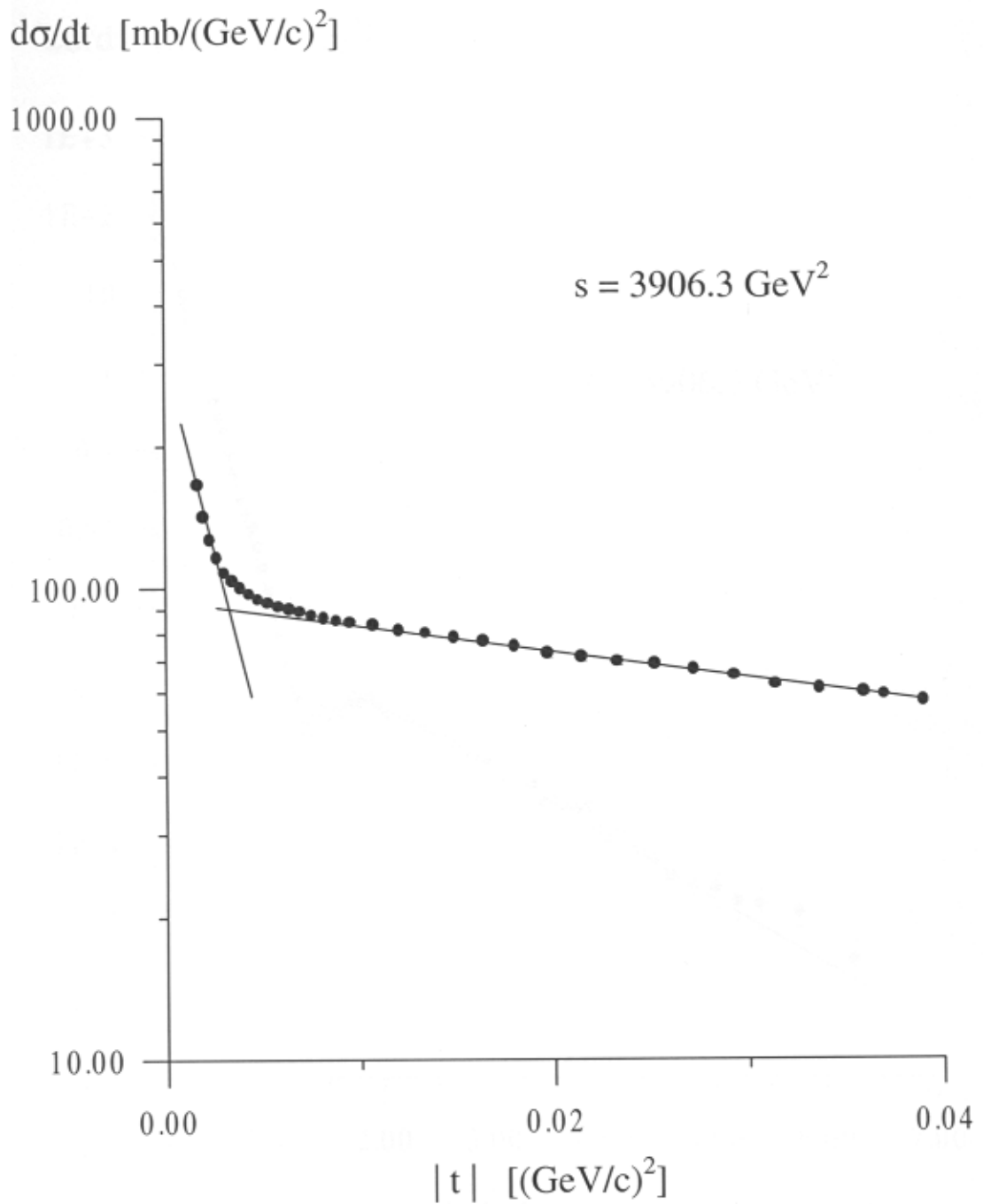
2.1 Nucleon Structure and Nucleon-Nucleon Interaction

The only way to study into the detailed structure of nucleon is to bombard particles (usually of smaller size) onto nucleons, then collect and analyze

the scattered particles. The higher the incident energy of the projectile has, the deeper structure of nucleon would be revealed. The subtle structure of nucleon is mainly established in scattering experiments at high energies. Shown in Fig. 2.1 is the observed invariant differential cross section, $d\sigma/dt$ of the proton-proton elastic scattering at an energy $s = 3906.3 \text{ GeV}^2$ (see Appendix A for the definitions of Mandelstam variables s , t and u). It is clearly seen in the plots in Fig. 2.1 that there exist three different slopes at different regions of $|t|$ values, which may indicate that the proton has compound structure.

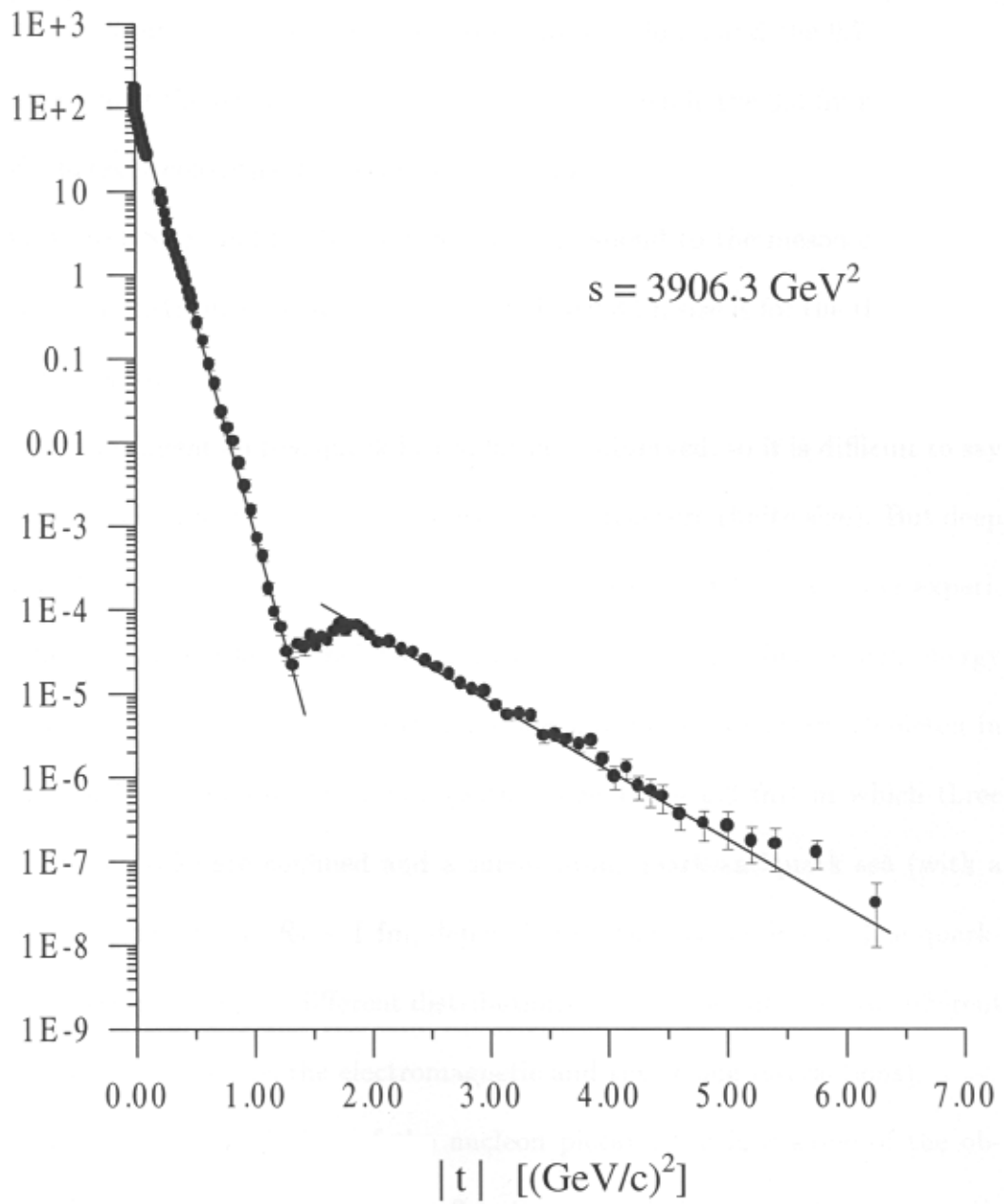
At very low momentum transfer regime (very small $|t|$) shown in Fig. 2.1(a), the interaction is mainly the electromagnetic interaction. Thus, the slope at very small $|t|$ corresponds to the proton electric and magnetic form factors which have been well established in high energy electron-proton collisions. A size parameter of proton extracted from the proton electric form factor is about 0.8 fm.

The electromagnetic interaction contribution drops to $\sim 1\%$ of the observed differential cross section, so the second slope ($0.01 < |t| < 1.5 \text{ (GeV/c)}^2$) stems mainly from the strong interaction. The experimental data analysis results in a size parameter of proton around 0.7 fm. At large momentum transfer ($|t| > 1.5 \text{ (GeV/c)}^2$), the third slope is observed, which is, of course, due to the strong interaction, and corresponds to a proton size about 0.3 fm.



(a)

Figure 2.1 The plots of $d\sigma/dt$ vs. $|t|$ at $s = 3906.3 \text{ GeV}^2$ (a) in the small $|t|$ region and (b) in the large $|t|$ region. The solid lines just for eyes-guidance to the different slopes. Data are taken from Schopper (ed.), 1980, pp.284-286.

$d\sigma/dt$ [mb/(GeV/c)²]

(b)

Figure 2.1 (continued)

Theoretical understandings of the slopes mentioned above, or the size parameters, fall mainly into two groups:

- (i) The 0.8 fm proton size corresponds to the meson cloud, and the 0.7 fm size to the outer size of the proton (the bag of three quarks) while the 0.3 fm may be the size of whatever constituents the proton contains.
- (ii) Both the 0.8 fm and 0.7 fm proton sizes correspond to the meson clouds, but with different distributions (see Chapter IV). The 0.3 fm size is for the three-quark core of the proton.

In experiment no free quark has so far been observed, so it is difficult to say that quarks are point-like objects or objects with structure (finite size). But deep inelastic electron-nucleon, neutron-nucleon and nucleon-nucleon collision experiments favor that quarks are point-like. Based on a large number of high energy elastic and inelastic reactions, we may picture nucleon as an object depicted in Fig.2.2, which is composed of a core (with a size $R_1 \sim 0.3$ fm) in which three quarks of point-like are confined and a surrounding quark-antiquark sea (with a root-mean-square radius $R_2 \sim 1$ fm, depending on the interactions). The quark-antiquark sea may present different distributions hence different sizes for different interactions (for example, the electromagnetic and the strong interactions).

From our point of view of the nucleon picture, the first slope of the observed differential cross section in Fig. 2.1 stems mainly from the electromagnetic interaction of the quark-antiquark sea and the second slope is mainly contributed by the strong interaction of the quark-antiquark sea while the third slope in the large momentum transfer region might be due to both the quark-antiquark sea interaction and quark-gluon interaction. In our work, the quark-antiquark strong

interaction is parameterized as meson exchanges.

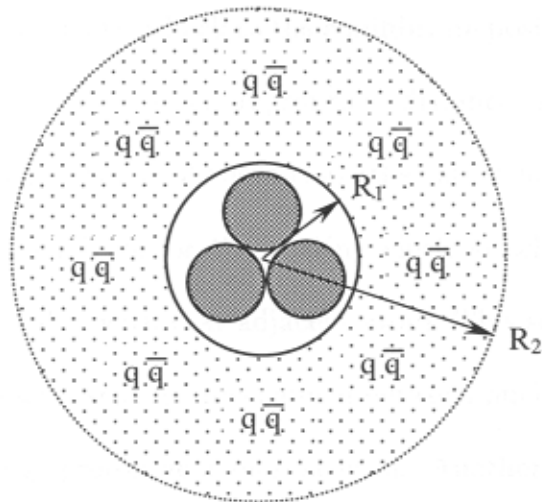


Figure 2.2 The picture represents the detail structure of the nucleon.

2.2 Meson Exchange in Strong Interaction

First, let us see some important evidences from the observation in nuclear experiments. Those evidences did historically hint that the meson exchange is at least an effective mechanism that responsible for the nuclear strong interaction.

(i) The saturation of nuclear force within nuclei: It is well known that the distribution of nuclear matter within nuclei is fairly uniform up to the edge of the nuclei. Also, the binding energy per nucleon is relatively constant in intermediate and heavy nuclei. This means that nucleon interacts to the other neighboring nucleons in the manner that if there are too much separation, they attract each other, and when they are too close they repel. The final result is the saturated configuration of the nucleon distribution in nuclei. The reminiscent to the situation in atomic physics is the forming of a diatomic molecule from two atoms by covalent bonding. These two atoms share the electrons (exchange of electrons between these

two atoms) by keeping the separation between them at a certain distance. If they are too close, they repel each other back to the equilibrium position. If they are too far away, they attract each other to an appropriate distance. At the equilibrium, the molecule is saturated. That is, if there is another atom nearby this molecule, since there is no room available for the sharing electron scheme to occur, this molecule will interact weakly with that adjacent atom. This situation gave us the confidence about the meson exchange mechanism between nucleons within nuclei.

(ii) The high energy proton-neutron scattering: Another important evidence for the meson exchange in the strong interaction between nucleons came from the high energy proton-neutron scattering experiments, see Stone, Chanowski, Gray, Gustafson, Jones, and Longo (1977). There is always a strong backward peak (scattering angle $\theta \sim 180^\circ$) in the differential cross section. It seems impossible since there is no identity effect as in proton-proton elastic scattering which ensure the backward-peak near 180° . However, this can be understood by using the meson exchange model to describe such process. The point is that the proton and neutron exchange something and result in changing of the positions between them. That is the incoming proton (neutron) becomes the outgoing neutron (proton). Thing exchanged by them must have charge in order to change the characteristics between those two nucleons. These charged-particles are the charged-mesons such as π^- or π^+ , etc. This process is known as “the charge exchange” (CEX).

The idea of meson exchange responsible for the strong interaction was first proposed by the Japanese physicist, Hideki Yukawa in 1935. The exchanged particle proposed by Yukawa has its mass lie between those of the electron and the nucleon. The idea for the strong interaction between nucleons is that one of the nucleons emits a particle, denoted by x

$$N_1 \rightarrow N_1 + x,$$

then another nucleon absorbs the particle x

$$N_2 + x \rightarrow N_2.$$

It is the same idea as that of photon exchange in the electromagnetic interaction. It is impossible in classical mechanics that the particle N_1 (N_2) emits (absorbs) another particle x without losing any energy. Fortunately, the uncertainty principle in quantum theory solves the problem by allowing the particle x to exist in the time interval, Δt .

In order to estimate the mass of particle x , let us assume further that particle x has a speed nearly to the speed of light, c . The distance that particle x can travel is

$$R = c\Delta t \approx \frac{\hbar c}{\Delta E} = \frac{\hbar c}{m_x c^2}, \quad (2.1)$$

where the uncertainty principle, $\Delta t \approx \frac{\hbar}{\Delta E}$, and the mass-energy relation for particle x , $\Delta E = m_x c^2$ are used. If we regard that the range of strong interaction between nucleons is roughly about the size of the nucleon, say $R \sim 1$ fm, by following this scheme we can roughly deduce that the mass of the particle x is

$$m_x \approx 200 \text{ MeV}. \quad (2.2)$$

Since this mass lies between the mass of the electron and the nucleon. The particle x is called “meson”, precisely π -meson or pion. (From the Greek word “meso” which means middle.) In 1936, one year after the Yukawa’s proposal, C.D. Anderson discovered such intermediate-mass particle in the cosmic ray experiment. However, this particle did not interact strongly with the nucleon and could not be the exchanged particle mentioned by Yukawa. This particle is actually known as “muon” and classified as a lepton, not as the meson. The success in finding the pion was accomplished in 1947 by C.F. Powell. This pion has the mass of about 140 MeV and has the same properties as Yukawa predicted. Due to the fantastic idea that the exchange pion is responsible for the strong interaction, Yukawa was awarded the Nobel Prize in Physics in 1949.

The model originally proposed by Yukawa has been extended by many physicists over decades. Not only pion is included in the model, but the heavier mesons like ω - and ρ -mesons and even multiple meson-exchanges are also included as reviewed in the work of Machleidt et al. (1987).

In next chapter, we will start to construct the transition amplitudes for the proton-proton elastic scattering from the relevant Feynman diagrams.

Chapter III

Formulation

In Chapter II, we have introduced the idea of exchanging massive particle in strong interaction. We are now ready to construct, from the Feynman diagram, the transition amplitude, hence the differential cross section, for the proton-proton scattering process based on the meson exchange model. First of all, we will make our conventions in the framework of the center of mass system. In order to construct such transition amplitude, all we need to know is the interaction Lagrangians for the system of the exchanged-particle and the proton. In this work, we consider the electromagnetic and strong interactions for the proton-proton elastic scattering process. As for the strong interaction, it is believed that the sea-quark interaction is dominant over the direct quark-gluon one since the process is elastic. The sea-quark interaction is parameterized to the meson-exchange processes in the work. In principle one should include all the mesons which have a strong coupling to nucleon, but in this work we consider only the lightest and the second lightest mesons. Our preliminary study suggests that the important particles for the proton-proton interaction are the mesons $\pi(140)$, $\omega(780)$, $\sigma(980)$, $\rho(770)$, $f_2(1270)$, and $\omega(1420)$ (the numbers in the parentheses represent the rest masses of the particles in unit of MeV/c^2).

Since the proton-proton elastic scattering includes the identity particle effect, one must consider both the direct diagram and the cross diagrams in the Feynman diagrams, as shown in Fig. 3.1. The total transition amplitude is the sum of the transition amplitudes for all of the meson-exchange diagrams, both the direct and the cross ones. Then, the invariant differential cross section $d\sigma/dt$ can be deduced from the total transition amplitude.

There are two classes of free parameters involved in this work, that is, the coupling constants and the cutoff parameters. A coupling constant tells us how strong the interaction mediated by a meson is while a cutoff parameter contains the information of the size of proton. These unknown parameters will be determined by fitting with the experimental data at a large energy regime from $s \approx 500$ to $s \approx 4000 \text{ GeV}^2$.

First, we will start with a discussion of the two-particle scattering process in the center of mass system, then come to the derivation of the proton-proton elastic differential cross section. Finally, various Lagrangians and transition amplitudes will be worked out.

3.1 Center of Mass System

The Feynman diagrams of two-particle scattering processes

$$1 + 2 \rightarrow 3 + 4 \tag{3.1}$$

are shown in Fig. 3.1 (Fig. 3.1(b) should be included if the two incoming particles are identical) where p_i and λ_i represent respectively the energy-momentum four-vector and the spin of the i^{th} particles. The direction of the propagation in

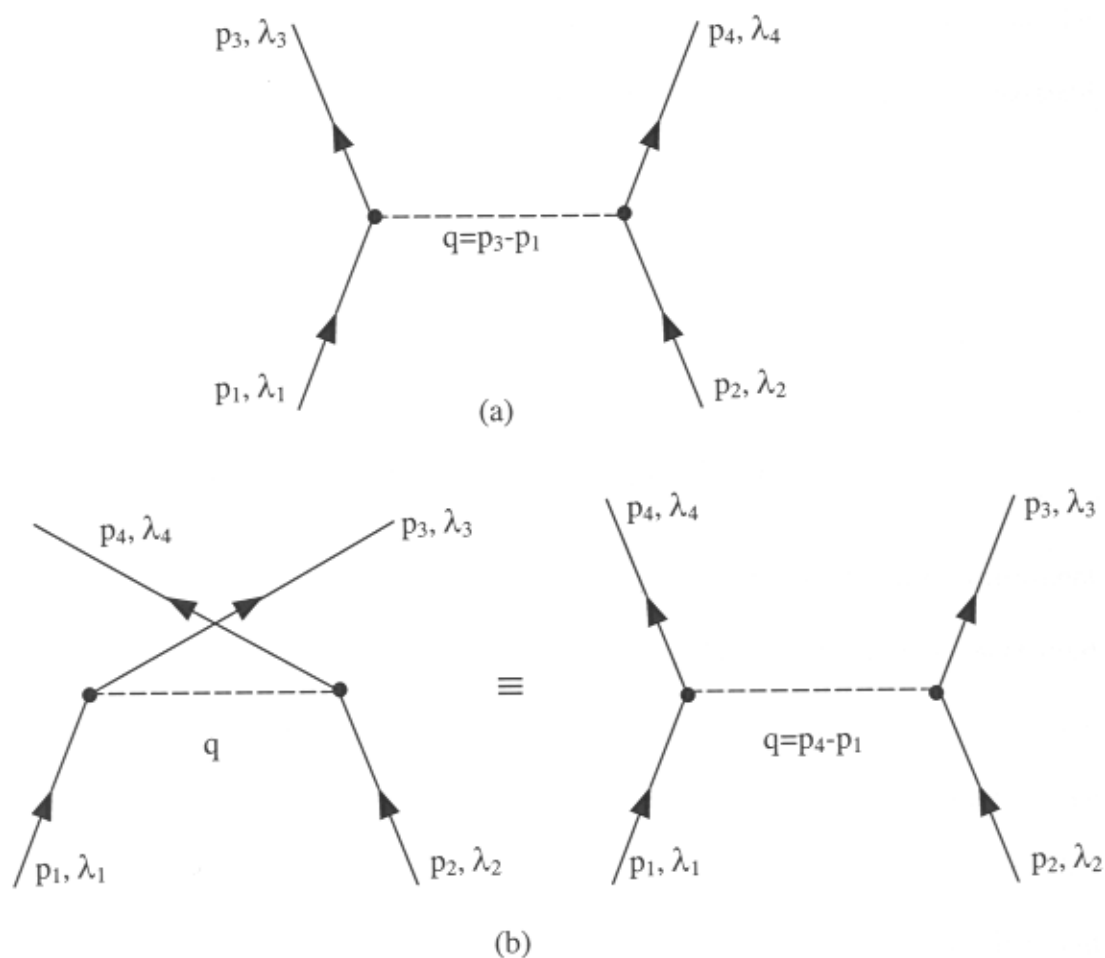


Figure 3.1 The Feynman diagrams for the proton-proton elastic scattering (a) the direct diagram and (b) the cross diagram.

time is chosen to be in the upward direction. For proton-proton elastic scattering, it is convenient to work in the center-of-mass (CM) system using the Mandelstam variables (see Appendix A). In the center-of-mass system, the Feynman diagrams in Fig. 3.1(a) and 3.1(b) correspond respectively to the reactions illustrated in Fig. 3.2(a) (the direct process) and in Fig. 3.2(b) (the cross process). Since the two protons involved are identical, one has no chance in experiments to distinguish whether the particle observed in the direction θ is initially the particle 1 or

the particle 2. In practical calculation, a coordinate system is chosen so that the scattering plane is the x - z plane and the momentum \vec{p}_1 of the incoming particle 1 is in the $+z$ direction. Therefore, in the CM system, the incoming particle 2 has the momentum \vec{p}_2 in the $-z$ direction with the same magnitude as that of the particle 1, that is, $\vec{p}_1 = -\vec{p}_2$.

3.2 The Differential Cross Section

One of the important observables extracted from the scattering experiment is the differential cross section which tells us the probability to find the scattered particles of certain states in a particular direction of space. The total cross section (derived theoretically by integrating the differential cross section over angles) which is the probability to find the scattered particles of certain states in all the direction might be understood as the effective size of the target as seen by the incident particle. Therefore, from the knowledge of cross sections one may extract the size of particles involved in a scattering process. The cross section, $d\sigma$, is defined in the symbolic form as

$$d\sigma = \frac{|T|^2}{F} dQ, \quad (3.2)$$

where T is the invariant amplitude which is directly related to the S-matrix.

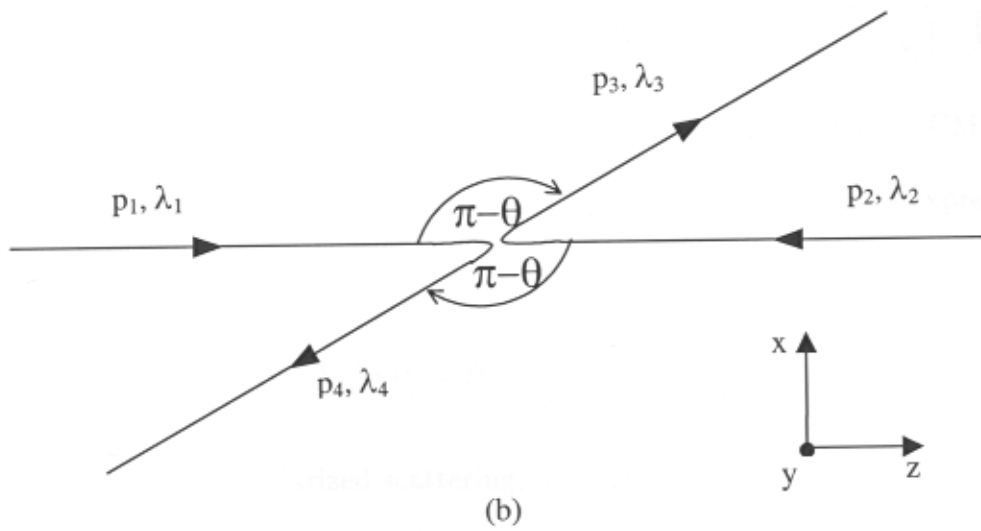
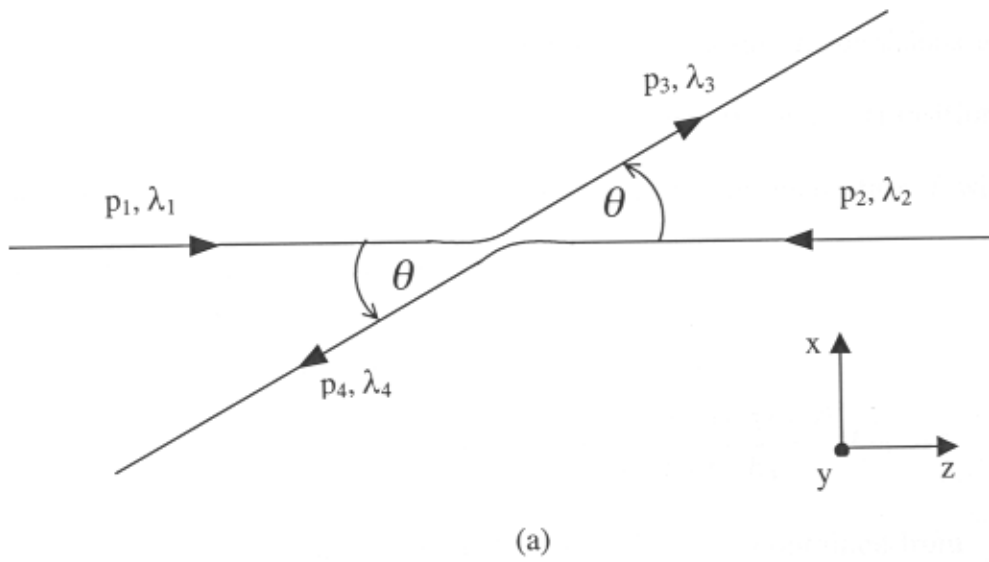


Figure 3.2 The CM system for the elastic scattering process $1 + 2 \rightarrow 3 + 4$, (a) the direct diagram and (b) the cross diagram.

For the proton-proton scattering and the normalization conditions used in this work (see Appendix B), the element of the S-matrix for the transition from initial state i with the total energy-momentum P_i to the final state f with the total energy-momentum P_f can be expressed as

$$\begin{aligned} S_{fi} &= \langle f | S | i \rangle \\ &= \delta_{fi} - \frac{i}{(2\pi)^2} \delta^{(4)}(P_f - P_i) \left(\frac{M}{E_1} \frac{M}{E_2} \frac{M}{E_3} \frac{M}{E_4} \right)^{1/2} T_{fi}, \end{aligned} \quad (3.3)$$

where M is the proton mass. The incident flux, F , can be obtained from

$$F = |\vec{v}_1 - \vec{v}_2| \frac{E_1 E_2}{M M}. \quad (3.4)$$

Note that, this definition of F works for the collinear scattering such as in CM system. The Lorentz invariant phase space factor, dQ , (also called dLips) is expressed by

$$dQ = (2\pi)^4 \delta^{(4)}(P_f - P_i) \frac{M d^3 p_3}{E_3 (2\pi)^3} \frac{M d^3 p_4}{E_4 (2\pi)^3}. \quad (3.5)$$

In the case of unpolarized scattering, one has

$$|T|^2 \rightarrow \frac{1}{4} \sum_{\lambda_1 \lambda_2 \lambda_3 \lambda_4} |T_{fi}|^2, \quad (3.6)$$

where T_{fi} is defined by

$$\begin{aligned} T_{fi} &= \langle f | T | i \rangle \\ &= \langle \lambda_3 \lambda_4 | T | \lambda_1 \lambda_2 \rangle. \end{aligned} \quad (3.7)$$

From (3.2), (3.4), and (3.5), the unpolarized differential cross section $d\sigma/d\Omega$ for the proton-proton elastic scattering is derived as (see also Appendix C)

$$\frac{d\sigma}{d\Omega} = \frac{1}{(4\pi)^2} \frac{M^4}{E^2} \frac{1}{4} \sum_{\lambda_1 \lambda_2 \lambda_3 \lambda_4} |T_{fi}|^2, \quad (3.8)$$

where E is the energy of the projectile. In term of variable t , the differential cross section, $d\sigma/dt$, can be obtained from (3.8) by

$$\begin{aligned} \frac{d\sigma}{dt} &= \frac{\pi}{p^2} \frac{d\sigma}{d\Omega} \\ &= \frac{1}{(4\pi)^2} \frac{M^4}{E^2} \frac{\pi}{4p^2} \sum_{\lambda_1 \lambda_2 \lambda_3 \lambda_4} |T_{fi}|^2. \end{aligned} \quad (3.9)$$

Since there are two possible spin-states for each proton, there are totally sixteen possible configurations for T_{fi} . We need to consider all these sixteen terms. Due to the special invariant properties for the NN interaction, namely, the parity conservation, the conservation of total spin, and the time-reversal, we can reduce these sixteen terms to only five terms which are linearly independent. The parity conservation leads to

$$\langle \lambda_3 \lambda_4 | T | \lambda_1 \lambda_2 \rangle = \langle -\lambda_3, -\lambda_4 | T | -\lambda_1, -\lambda_2 \rangle,$$

the conservation of total spin leads to

$$\langle \lambda_3 \lambda_4 | T | \lambda_1 \lambda_2 \rangle = \langle \lambda_4 \lambda_3 | T | \lambda_2 \lambda_1 \rangle,$$

and the time-reversal leads to

$$\langle \lambda_3 \lambda_4 | T | \lambda_1 \lambda_2 \rangle = \langle \lambda_1 \lambda_2 | T | \lambda_3 \lambda_4 \rangle.$$

By using the above symmetries, the sixteen terms can be classified as

$$T_1 = \langle ++ | T | ++ \rangle = \langle -- | T | -- \rangle,$$

$$T_2 = \langle ++ | T | -- \rangle = \langle -- | T | ++ \rangle,$$

$$T_3 = \langle +- | T | +- \rangle = \langle -+ | T | -+ \rangle,$$

$$T_4 = \langle +- | T | -+ \rangle = \langle -+ | T | +- \rangle,$$

$$\begin{aligned}
T_5 &= \langle ++ | T | +- \rangle = \langle ++ | T | -+ \rangle = \langle +- | T | ++ \rangle = \langle +- | T | -- \rangle \\
&= \langle -+ | T | ++ \rangle = \langle -+ | T | -- \rangle = \langle -- | T | -+ \rangle = \langle -- | T | +- \rangle,
\end{aligned}$$

where + (-) denotes the spin up (down) state. Therefore, (3.9) can be rewritten as

$$\frac{d\sigma}{dt} = \frac{1}{(4\pi)^2} \frac{M^4}{E^2} \frac{\pi}{4p^2} [2(|T_1|^2 + |T_2|^2 + |T_3|^2 + |T_4|^2 + 4|T_5|^2)], \quad (3.10)$$

or in terms of the Mandelstam variables

$$\frac{d\sigma}{dt} = \frac{1}{4\pi s(s-4M^2)} [2(|T_1|^2 + |T_2|^2 + |T_3|^2 + |T_4|^2 + 4|T_5|^2)]. \quad (3.11)$$

All that we need to compute are $T_1, T_2, T_3, T_4,$ and T_5 , only one for each term, for example;

$$T_1 = \langle ++ | T | ++ \rangle,$$

$$T_2 = \langle ++ | T | -- \rangle,$$

$$T_3 = \langle +- | T | +- \rangle,$$

$$T_4 = \langle +- | T | -+ \rangle,$$

$$T_5 = \langle ++ | T | +- \rangle.$$

The way to compute these terms is the subject of next section.

3.3 Lagrangian

The Lagrangian for the system considered here may be written as

$$\mathcal{L} = \mathcal{L}_N + \mathcal{L}_\gamma + \mathcal{L}_s + \mathcal{L}_{ps} + \mathcal{L}_v + \mathcal{L}_{NN\gamma} + \mathcal{L}_{NNs} + \mathcal{L}_{NNps} + \mathcal{L}_{NNv},$$

where \mathcal{L}_N , \mathcal{L}_γ , \mathcal{L}_s , \mathcal{L}_{ps} , and \mathcal{L}_v are free Lagrangians for nucleon, γ , scalar meson, pseudoscalar meson, and vector meson, respectively. The interaction Lagrangians, $\mathcal{L}_{NN\gamma}$, \mathcal{L}_{NNs} , \mathcal{L}_{NNps} , and \mathcal{L}_{NNv} are for the $NN\gamma$, NNs , $NNps$, and NNv coupling, respectively.

The general form of the interaction Lagrangians, as mentioned in the work of Machleidt et al. (1987), for the interactions between nucleons and mediated meson can be written as

$$\mathcal{L}_{NNs} = g_s \bar{\psi} \psi \phi_s, \quad (3.12)$$

$$\mathcal{L}_{NNps} = \frac{f_{ps}}{m_{ps}} \bar{\psi} \gamma^5 \gamma^\mu \psi \partial_\mu \phi_{ps}, \quad (3.13)$$

$$\mathcal{L}_{NNv} = g_v \bar{\psi} \gamma_\mu \psi \phi_v^\mu + \frac{f_v}{4m} \bar{\psi} \sigma_{\mu\nu} \psi (\partial^\mu \phi_v^\nu - \partial^\nu \phi_v^\mu), \quad (3.14)$$

where \mathcal{L}_{NNs} , \mathcal{L}_{NNps} , and \mathcal{L}_{NNv} are the interaction Lagrangians density for the nucleons-scalar meson (spin-0 meson with even parity), nucleons-pseudoscalar meson (spin-0 meson with odd parity) and nucleons-vector meson (spin-1 meson with odd parity) interactions, respectively. Since proton is a charged-particle, the electromagnetic interaction should also be considered as well as the strong interaction. We will first study the proton-proton electromagnetic interaction Lagrangian, then introduce the interactions for the proton-proton-meson systems, one by one, from

the lowest to the highest masses of the mesons involved. Shown in Table 3.1 are some properties of the mesons involved in this work.

It is tedious (if not hard) to explicitly work out the differential cross section $d\sigma/dt$ since we consider the one-body exchanges of photon and six mesons, which leads to a large number of cross terms. For the complete version of the differential cross section, we would just interpret the total amplitude in terms of the Dirac four-spinors, propagators and form factors. The tedious calculation of the differential cross section from the amplitudes will be left to the computational calculation which gives rise to the same result obtained by hand, but much more easier.

Table 3.1 Properties of selected mesons in this work*

Particle	mass [MeV]	$I^G(J^{PC})$
π	140	$1^-(0^-+)$
ρ	770	$1^+(1^{--})$
ω	780	$0^-(1^{--})$
σ	980	$0^+(0^{++})$
f_2	1270	$0^+(2^{++})$
ω	1420	$0^-(1^{--})$

*Note Particle Data Group, Review of Particle Physics, Eur. Phys. J. C **3**, 1998.

3.3.1 Photon Exchange

For the electron-photon-electron interaction, as shown in Fig. 3.3(a), the current is simply

$$j^\mu = -e\bar{u}(p')\gamma^\mu u(p). \quad (3.15)$$

But for the proton-photon-proton interaction shown in Fig. 3.3(b), since proton has structure, one must use a modified form of the above current. The current for the proton-photon-proton interaction may take the form (see Appendix D for details)

$$J^\mu = e\bar{u}(p')\left[(F_1 + F_2)\gamma^\mu - \frac{F_2}{2M}(p^\mu + p'^\mu)\right]u(p), \quad (3.16)$$

where M is the proton mass, F_1 and F_2 are independent form factors related to the electric form factor $G_E(q^2)$ and the magnetic form factor $G_M(q^2)$ by

$$G_E(q^2) = F_1 + \frac{q^2}{4M^2}F_2, \quad (3.17)$$

$$G_M(q^2) = F_1 + F_2, \quad (3.18)$$

where q^2 is the square of the momentum transfer. The proton electric and magnetic form factors are well established by the experiments. The explicit form of the $G_E(q^2)$ is (see Griffiths, 1987, p. 267)

$$G_E(q^2) = \left(1 - \frac{q^2}{0.71}\right)^{-2} \quad (3.19)$$

$G_M(q^2)$ has the same form as $G_E(q^2)$ except a multiple constant, that is

$$G_M(q^2) = \mu G_E(q^2) = (1 + \kappa)G_E(q^2). \quad (3.20)$$

κ is the anomalous magnetic moment. The value of κ_p is 1.79 for the proton and κ_n is -1.91 for the neutron.

Follow the standard Feynman rules and use the current in (3.16) and the photon propagator in the Feynman gauge,

$$\Delta_{\mu\nu}(q^2) = \frac{-ig_{\mu\nu}}{q^2}, \quad (3.21)$$

one can easily write the amplitude, in term of Mandelstam variables, for both the direct diagram and the cross diagram, as follows

$$\begin{aligned} T_\gamma^{direct} &= \frac{e^2}{t} [\bar{u}_3(p_3, \lambda_3) \Gamma_{1\mu} u_1(p_1, \lambda_1)] [\bar{u}_4(p_4, \lambda_4) \Gamma_2^\mu u_2(p_2, \lambda_2)], \\ T_\gamma^{cross} &= \frac{e^2}{u} [\bar{u}_4(p_4, \lambda_4) \Gamma_{3\mu} u_1(p_1, \lambda_1)] [\bar{u}_3(p_3, \lambda_3) \Gamma_4^\mu u_2(p_2, \lambda_2)], \end{aligned}$$

with the vertex functions

$$\begin{aligned} \Gamma_{1\mu} &= (F_1 + F_2) \gamma_\mu - \frac{F_2}{2M} (p_{1\mu} + p_{3\mu}), \\ \Gamma_{2\mu} &= (F_1 + F_2) \gamma_\mu - \frac{F_2}{2M} (p_{2\mu} + p_{4\mu}), \\ \Gamma_{3\mu} &= (F_1 + F_2) \gamma_\mu - \frac{F_2}{2M} (p_{1\mu} + p_{4\mu}), \\ \Gamma_{4\mu} &= (F_1 + F_2) \gamma_\mu - \frac{F_2}{2M} (p_{2\mu} + p_{3\mu}). \end{aligned}$$

Thus, the total amplitude of the first-order proton-proton electromagnetic interaction is

$$\begin{aligned} T_\gamma &= T_\gamma^{direct} + T_\gamma^{cross} \\ &= \frac{e^2}{t} [\bar{u}_3(p_3, \lambda_3) \Gamma_{1\mu} u_1(p_1, \lambda_1)] [\bar{u}_4(p_4, \lambda_4) \Gamma_2^\mu u_2(p_2, \lambda_2)] \\ &\quad - \frac{e^2}{u} [\bar{u}_4(p_4, \lambda_4) \Gamma_{3\mu} u_1(p_1, \lambda_1)] [\bar{u}_3(p_3, \lambda_3) \Gamma_4^\mu u_2(p_2, \lambda_2)]. \quad (3.22) \end{aligned}$$

The presence of the minus sign in the second term is due to the interchange of the identical protons.

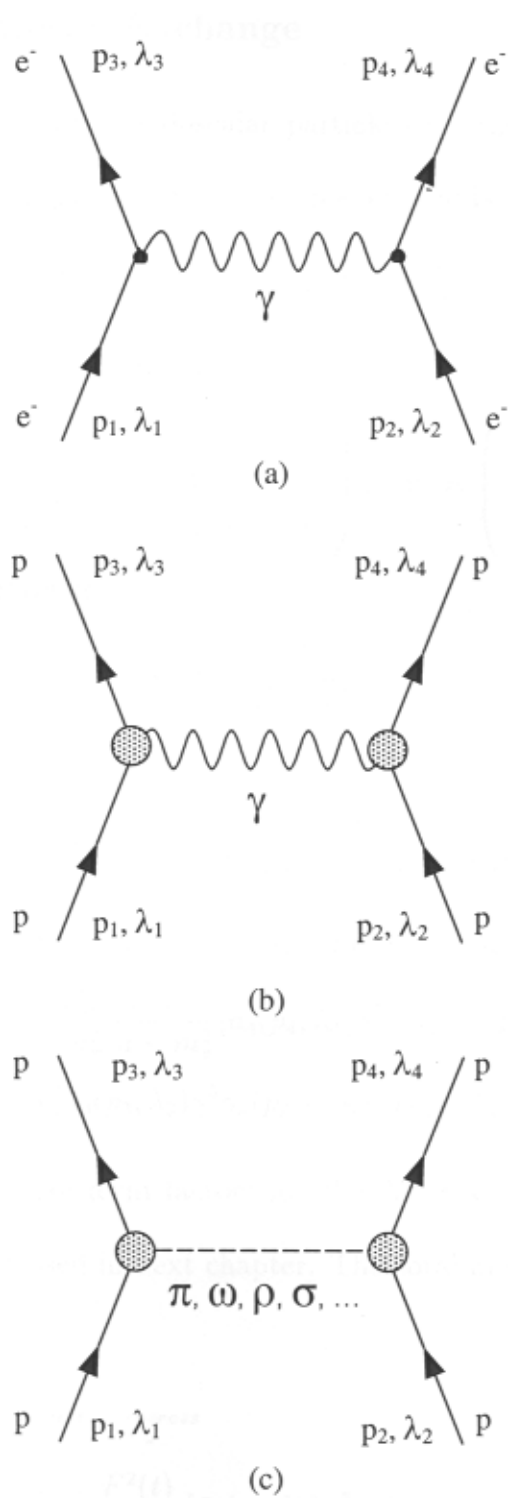


Figure 3.3 (a) $e^- e^- \gamma$ vertex in $e^- + e^- \rightarrow e^- + e^-$, (b) $pp\gamma$ vertex in electromagnetic interaction in $p + p \rightarrow p + p$, and (c) pp -meson vertex in strong interaction in meson-exchange model.

3.3.2 π Meson Exchange

π meson is a pseudoscalar particle with the mass $m_\pi = 140$ MeV.

The interaction Lagrangian for the π -meson exchange is

$$\mathcal{L}_{NN\pi} = \frac{g_{NN\pi}}{m_\pi} \bar{\psi} \gamma^5 \gamma^\mu \vec{\tau} \psi \cdot \partial_\mu \vec{\phi}_\pi, \quad (3.23)$$

where $\vec{\tau} = (\tau^1, \tau^2, \tau^3)$ are the Pauli matrices

$$\tau^1 = \begin{pmatrix} 0 & 1 \\ 1 & 0 \end{pmatrix}, \quad \tau^2 = \begin{pmatrix} 0 & -i \\ i & 0 \end{pmatrix}, \quad \tau^3 = \begin{pmatrix} 1 & 0 \\ 0 & -1 \end{pmatrix} \quad (3.24)$$

The π meson propagator is

$$\Delta(q) = \frac{i}{q^2 - m_\pi^2}. \quad (3.25)$$

The amplitudes obtained from the above Lagrangian and propagator are

$$\begin{aligned} T_\pi^{direct} &= -\frac{g_{pp\pi}^2}{m_\pi^2} \frac{F_\pi^2(t)}{t - m_\pi^2} [\bar{u}_3(p_3, \lambda_3) \gamma^5 \gamma_\mu (p_1 - p_3)^\mu u_1(p_1, \lambda_1)] \\ &\quad \times [\bar{u}_4(p_4, \lambda_4) \gamma^5 \gamma_\nu (p_2 - p_4)^\nu u_2(p_2, \lambda_2)], \\ T_\pi^{cross} &= -\frac{g_{pp\pi}^2}{m_\pi^2} \frac{F_\pi^2(u)}{u - m_\pi^2} [\bar{u}_4(p_4, \lambda_4) \gamma^5 \gamma_\mu (p_1 - p_4)^\mu u_1(p_1, \lambda_1)] \\ &\quad \times [\bar{u}_3(p_3, \lambda_3) \gamma^5 \gamma_\nu (p_2 - p_3)^\nu u_2(p_2, \lambda_2)], \end{aligned}$$

where $F(t)$ and $F(u)$ are form factors for the $NN\pi$ system. The form of $F(t)$ and $F(u)$ will be discussed in next chapter. The total amplitude for the π meson exchange is thus

$$\begin{aligned} T_\pi &= T_\pi^{direct} + T_\pi^{cross} \\ &= -\frac{g_{pp\pi}^2}{m_\pi^2} \frac{F^2(t)}{t - m_\pi^2} [\bar{u}_3(p_3, \lambda_3) \gamma^5 \gamma_\mu (p_1 - p_3)^\mu u_1(p_1, \lambda_1)] \\ &\quad \times [\bar{u}_4(p_4, \lambda_4) \gamma^5 \gamma_\nu (p_2 - p_4)^\nu u_2(p_2, \lambda_2)] \\ &\quad + \frac{g_{pp\pi}^2}{m_\pi^2} \frac{F^2(u)}{u - m_\pi^2} [\bar{u}_4(p_4, \lambda_4) \gamma^5 \gamma_\mu (p_1 - p_4)^\mu u_1(p_1, \lambda_1)] \\ &\quad \times [\bar{u}_3(p_3, \lambda_3) \gamma^5 \gamma_\nu (p_2 - p_3)^\nu u_2(p_2, \lambda_2)]. \end{aligned} \quad (3.26)$$

3.3.3 ρ Meson Exchange

ρ meson is a vector particle with the mass $m_\rho = 770$ MeV. The interaction Lagrangian for the ρ -meson exchange is

$$\begin{aligned} \mathcal{L}_{NN\rho} = & g_{NN\rho} \bar{\psi} \gamma_\mu \vec{\tau} \cdot \vec{\phi}_\rho^\mu \psi + \frac{1}{4M} g'_{NN\rho} \bar{\psi} \sigma_{\mu\nu} \\ & \times (\partial^\mu \vec{\phi}_\rho^\nu - \partial^\nu \vec{\phi}_\rho^\mu) \cdot \vec{\tau} \psi \end{aligned} \quad (3.27)$$

with the propagator

$$\Delta_{\mu\nu}(q) = \frac{-i}{q^2 - m_\rho^2} (g_{\mu\nu} - \frac{q_\mu q_\nu}{m_\rho^2}). \quad (3.28)$$

Assuming that, we can neglect the last term on the right hand side of (3.28), in the presence of the form factors, since it is an “off-mass shell” term which is expected to have no contribution to the differential cross section. Therefore, the amplitudes are

$$\begin{aligned} T_\rho^{direct} &= g_{pp\rho}^2 \frac{F_\rho^2(t)}{t - m_\rho^2} [\bar{u}_3(p_3, \lambda_3) \bar{\Gamma}_{1\mu} u_1(p_1, \lambda_1)] \\ &\quad \times [\bar{u}_4(p_4, \lambda_4) \bar{\Gamma}_2^\mu u_2(p_2, \lambda_2)], \\ T_\rho^{cross} &= g_{pp\rho}^2 \frac{F_\rho^2(u)}{u - m_\rho^2} [\bar{u}_4(p_4, \lambda_4) \bar{\Gamma}_{3\mu} u_1(p_1, \lambda_1)] \\ &\quad \times [\bar{u}_3(p_3, \lambda_3) \bar{\Gamma}_4^\mu u_2(p_2, \lambda_2)], \end{aligned}$$

where the vertex factors $\bar{\Gamma}_{1\mu}$, $\bar{\Gamma}_{2\mu}$, $\bar{\Gamma}_{3\mu}$, and $\bar{\Gamma}_{4\mu}$ are (see also Appendix D)

$$\begin{aligned} \bar{\Gamma}_{1\mu} &= (1 + f_{pp\rho}) \gamma_\mu - \frac{f_{pp\rho} (p_1 + p_3)_\mu}{2M}, \\ \bar{\Gamma}_{2\mu} &= (1 + f_{pp\rho}) \gamma_\mu - \frac{f_{pp\rho} (p_2 + p_4)_\mu}{2M}, \\ \bar{\Gamma}_{3\mu} &= (1 + f_{pp\rho}) \gamma_\mu - \frac{f_{pp\rho} (p_1 + p_4)_\mu}{2M}, \\ \bar{\Gamma}_{4\mu} &= (1 + f_{pp\rho}) \gamma_\mu - \frac{f_{pp\rho} (p_2 + p_3)_\mu}{2M}, \end{aligned}$$

and $f_{pp\rho} = g'_{pp\rho}/g_{pp\rho}$. The total amplitude for the ρ meson exchange is thus

$$\begin{aligned}
T_\rho &= T_\rho^{\text{direct}} + T_\rho^{\text{cross}} \\
&= g_{pp\rho}^2 \frac{F_\rho^2(t)}{t - m_\rho^2} [\bar{u}_3(p_3, \lambda_3) \bar{\Gamma}_{1\mu} u_1(p_1, \lambda_1)] [\bar{u}_4(p_4, \lambda_4) \bar{\Gamma}_2^\mu u_2(p_2, \lambda_2)] \\
&\quad - g_{pp\rho}^2 \frac{F_\rho^2(u)}{u - m_\rho^2} [\bar{u}_4(p_4, \lambda_4) \bar{\Gamma}_{3\mu} u_1(p_1, \lambda_1)] \\
&\quad \times [\bar{u}_3(p_3, \lambda_3) \bar{\Gamma}_4^\mu u_2(p_2, \lambda_2)]. \tag{3.29}
\end{aligned}$$

3.3.4 ω Meson Exchange

ω meson is a vector particle with the mass $m_\omega = 780$ MeV. The interaction Lagrangian for the ω exchange is

$$\mathcal{L}_{pp\omega} = g_{pp\omega} \bar{\psi} \gamma_\mu \phi_\omega \psi \tag{3.30}$$

with the propagator

$$\Delta_{\mu\nu}(q) = \frac{-i}{q^2 - m_\omega^2} (g_{\mu\nu} - \frac{q_\mu q_\nu}{m_\omega^2}). \tag{3.31}$$

The amplitudes are

$$\begin{aligned}
T_\omega^{\text{direct}} &= g_{pp\omega}^2 \frac{F_\omega^2(t)}{t - m_\omega^2} [\bar{u}_3(p_3, \lambda_3) \gamma_\mu u_1(p_1, \lambda_1)] [\bar{u}_4(p_4, \lambda_4) \gamma^\mu u_2(p_2, \lambda_2)], \\
T_\omega^{\text{cross}} &= g_{pp\omega}^2 \frac{F_\omega^2(u)}{u - m_\omega^2} [\bar{u}_4(p_4, \lambda_4) \gamma_\mu u_1(p_1, \lambda_1)] [\bar{u}_3(p_3, \lambda_3) \gamma^\mu u_2(p_2, \lambda_2)].
\end{aligned} \tag{3.32}$$

The total amplitude for the ω meson exchange is thus

$$\begin{aligned}
T_\omega &= T_\omega^{\text{direct}} + T_\omega^{\text{cross}} \\
&= g_{pp\omega}^2 \frac{F_\omega^2(t)}{t - m_\omega^2} [\bar{u}_3(p_3, \lambda_3) \gamma_\mu u_1(p_1, \lambda_1)] [\bar{u}_4(p_4, \lambda_4) \gamma^\mu u_2(p_2, \lambda_2)] \\
&\quad - g_{pp\omega}^2 \frac{F_\omega^2(u)}{u - m_\omega^2} [\bar{u}_4(p_4, \lambda_4) \gamma_\mu u_1(p_1, \lambda_1)] [\bar{u}_3(p_3, \lambda_3) \gamma^\mu u_2(p_2, \lambda_2)]. \tag{3.32}
\end{aligned}$$

3.3.5 σ Meson Exchange

σ meson (or f_0 meson) is a scalar particle with the mass of 980 MeV.

The interaction Lagrangian for the σ meson exchange is

$$\mathcal{L}_{pp\sigma} = g_{pp\sigma} \bar{\psi} \psi \phi_\sigma \quad (3.33)$$

with the propagator

$$\Delta(q) = \frac{i}{q^2 - m_\sigma^2}. \quad (3.34)$$

The amplitudes are

$$\begin{aligned} T_\sigma^{direct} &= -g_{pp\sigma}^2 \frac{F_\sigma^2(t)}{t - m_\sigma^2} [\bar{u}_3(p_3, \lambda_3) u_1(p_1, \lambda_1)] [\bar{u}_4(p_4, \lambda_4) u_2(p_2, \lambda_2)], \\ T_\sigma^{cross} &= -g_{pp\sigma}^2 \frac{F_\sigma^2(u)}{u - m_\sigma^2} [\bar{u}_4(p_4, \lambda_4) u_1(p_1, \lambda_1)] [\bar{u}_3(p_3, \lambda_3) u_2(p_2, \lambda_2)]. \end{aligned}$$

The total amplitude for the σ meson exchange is thus

$$\begin{aligned} T_\sigma &= T_\sigma^{direct} + T_\sigma^{cross} \\ &= -g_{pp\sigma}^2 \frac{F_\sigma^2(t)}{t - m_\sigma^2} [\bar{u}_3(p_3, \lambda_3) u_1(p_1, \lambda_1)] [\bar{u}_4(p_4, \lambda_4) u_2(p_2, \lambda_2)] \\ &\quad + g_{pp\sigma}^2 \frac{F_\sigma^2(u)}{u - m_\sigma^2} [\bar{u}_4(p_4, \lambda_4) u_1(p_1, \lambda_1)] [\bar{u}_3(p_3, \lambda_3) u_2(p_2, \lambda_2)]. \end{aligned} \quad (3.35)$$

3.3.6 $f_2(1270)$ Meson Exchange

f_2 meson is a spin-2 particle with the mass $m_{f_2} = 1270$ MeV. The interaction Lagrangian for the f_2 meson exchange is (Yan and Tegen, 1996)

$$\begin{aligned} \mathcal{L}_{NNf_2} &= i \frac{1}{2M} g_{NNf_2} (\bar{\psi} \gamma^\mu \partial^\nu \psi - \partial^\nu \bar{\psi} \gamma^\mu \psi) \phi_{f\mu\nu} + \frac{1}{2M^2} g'_{NNf_2} (\bar{\psi} \partial^\mu \partial^\nu \psi \\ &\quad - \partial^\mu \bar{\psi} \partial^\nu \psi - \partial^\nu \bar{\psi} \partial^\mu \psi + \partial^\mu \partial^\nu \bar{\psi} \psi) \phi_{f\mu\nu}. \end{aligned} \quad (3.36)$$

The propagator for f_2 is (Nath, 1965)

$$\begin{aligned} \Delta_{\mu\nu\rho\kappa}(q) = & \frac{i}{q^2 - m_{f_2}^2} [g_{\mu\rho}g_{\nu\kappa} + g_{\mu\kappa}g_{\nu\rho} - \frac{2}{3}g_{\mu\nu}g_{\rho\kappa} \\ & + (g_{\mu\rho}q_\nu q_\kappa + g_{\mu\kappa}q_\nu q_\rho + g_{\nu\rho}q_\mu q_\kappa + g_{\nu\kappa}q_\mu q_\rho \\ & - \frac{3}{2}g_{\mu\nu}q_\rho q_\kappa - \frac{3}{2}g_{\rho\kappa}q_\mu q_\nu) / m_{f_2}^2 + \frac{4}{3}q_\mu q_\nu q_\rho q_\kappa / m_{f_2}^4]. \end{aligned} \quad (3.37)$$

Supposing that only the first three terms in (3.37) contribute to the differential cross section, because of the same reason as for the vector boson, then the amplitudes are

$$\begin{aligned} T_{f_2}^{direct} &= -g_{ppf_2}^2 \frac{F_{f_2}^2(t)}{t - m_{f_2}^2} [\bar{u}_3(p_3, \lambda_3) \Gamma_{f_2}^{(1)\mu\nu} u_1(p_1, \lambda_1)] \\ &\quad \times \Delta_{\mu\nu\rho\kappa} [\bar{u}_4(p_4, \lambda_4) \Gamma_{f_2}^{(2)\rho\kappa} u_2(p_2, \lambda_2)], \\ T_{f_2}^{cross} &= -g_{ppf_2}^2 \frac{F_{f_2}^2(u)}{u - m_{f_2}^2} [\bar{u}_4(p_4, \lambda_4) \Gamma_{f_2}^{(3)\mu\nu} u_1(p_1, \lambda_1)] \\ &\quad \times \Delta_{\mu\nu\rho\kappa} [\bar{u}_3(p_3, \lambda_3) \Gamma_{f_2}^{(4)\rho\kappa} u_2(p_2, \lambda_2)], \end{aligned} \quad (3.39)$$

with the vertex factors for the f_2 meson exchange (see Appendix D)

$$\begin{aligned} \Gamma_{f_2}^{(1)\mu\nu} &= \frac{1}{2M} \gamma^\mu (p_1^\nu + p_3^\nu) - \frac{1}{2M^2} f_{ppf_2} (p_1^\mu p_1^\nu + p_3^\mu p_3^\nu + p_3^\mu p_1^\nu + p_1^\mu p_3^\nu), \\ \Gamma_{f_2}^{(2)\mu\nu} &= \frac{1}{2M} \gamma^\mu (p_2^\nu + p_4^\nu) - \frac{1}{2M^2} f_{ppf_2} (p_2^\mu p_2^\nu + p_4^\mu p_4^\nu + p_4^\mu p_2^\nu + p_2^\mu p_4^\nu), \\ \Gamma_{f_2}^{(3)\mu\nu} &= \frac{1}{2M} \gamma^\mu (p_1^\nu + p_4^\nu) - \frac{1}{2M^2} f_{ppf_2} (p_1^\mu p_1^\nu + p_4^\mu p_4^\nu + p_4^\mu p_1^\nu + p_1^\mu p_4^\nu), \\ \Gamma_{f_2}^{(4)\mu\nu} &= \frac{1}{2M} \gamma^\mu (p_2^\nu + p_3^\nu) - \frac{1}{2M^2} f_{ppf_2} (p_2^\mu p_2^\nu + p_3^\mu p_3^\nu + p_3^\mu p_2^\nu + p_2^\mu p_3^\nu), \end{aligned}$$

where $f_{ppf_2} = g'_{ppf_2} / g_{ppf_2}$. The total amplitude for the f_2 meson exchange is thus

$$\begin{aligned} T_{f_2} &= T_{f_2}^{direct} + T_{f_2}^{cross} \\ &= -g_{ppf_2}^2 \frac{F_{f_2}^2(t)}{t - m_{f_2}^2} [\bar{u}_3(p_3, \lambda_3) \Gamma_{f_2}^{(1)\mu\nu} u_1(p_1, \lambda_1)] \\ &\quad \times \Delta_{\mu\nu\rho\kappa} [\bar{u}_4(p_4, \lambda_4) \Gamma_{f_2}^{(2)\rho\kappa} u_2(p_2, \lambda_2)] \\ &\quad + g_{ppf_2}^2 \frac{F_{f_2}^2(u)}{u - m_{f_2}^2} [\bar{u}_4(p_4, \lambda_4) \Gamma_{f_2}^{(3)\mu\nu} u_1(p_1, \lambda_1)] \\ &\quad \times \Delta_{\mu\nu\rho\kappa} [\bar{u}_3(p_3, \lambda_3) \Gamma_{f_2}^{(4)\rho\kappa} u_2(p_2, \lambda_2)]. \end{aligned} \quad (3.38)$$

3.3.7 $\omega(1420)$ Meson Exchange

$\omega(1420)$ meson is a vector particle with the mass $M_\omega = 1420$ MeV.

The interaction Lagrangian for the $\omega(1420)$ meson exchange is the same as the $\rho(770)$ meson, except that the mass in the propagator must be changed from m_ρ to M_ω .

$$\begin{aligned} \mathcal{L}_{NN\omega(1420)} &= g_{NN\omega(1420)} i \bar{\psi} \gamma_\mu \vec{\tau} \cdot \vec{\phi}_{\omega(1420)}^\mu \psi + \frac{i}{4M} g'_{NN\omega(1420)} \bar{\psi} \sigma_{\mu\nu} \\ &\quad \times (\partial^\mu \vec{\phi}_{\omega(1420)}^\nu - \partial^\nu \vec{\phi}_{\omega(1420)}^\mu) \cdot \vec{\tau} \psi \end{aligned} \quad (3.39)$$

with the propagator

$$\Delta_{\mu\nu}(q) = \frac{-i}{q^2 - M_\omega^2} (g_{\mu\nu} - \frac{q_\mu q_\nu}{M_\omega^2}) \quad (3.40)$$

and the amplitudes are

$$\begin{aligned} T_{\omega(1420)}^{direct} &= g_{pp\omega(1420)}^2 \frac{F_{\omega(1420)}^2(t)}{t - M_\omega^2} [\bar{u}_3(p_3, \lambda_3) \Gamma'_{1\mu} u_1(p_1, \lambda_1)] \\ &\quad \times [\bar{u}_4(p_4, \lambda_4) \Gamma'_{2\mu} u_2(p_2, \lambda_2)], \\ T_{\omega(1420)}^{cross} &= g_{pp\omega(1420)}^2 \frac{F_{\omega(1420)}^2(u)}{u - M_\omega^2} [\bar{u}_4(p_4, \lambda_4) \Gamma'_{3\mu} u_1(p_1, \lambda_1)] \\ &\quad \times [\bar{u}_3(p_3, \lambda_3) \Gamma'_{4\mu} u_2(p_2, \lambda_2)] \end{aligned}$$

with the vertex factors

$$\begin{aligned} \Gamma'_{1\mu} &= (1 + f_{pp\omega(1420)}) \gamma_\mu - \frac{f_{pp\omega(1420)}(p_1 + p_3)_\mu}{2M}, \\ \Gamma'_{2\mu} &= (1 + f_{pp\omega(1420)}) \gamma_\mu - \frac{f_{pp\omega(1420)}(p_2 + p_4)_\mu}{2M}, \\ \Gamma'_{3\mu} &= (1 + f_{pp\omega(1420)}) \gamma_\mu - \frac{f_{pp\omega(1420)}(p_1 + p_4)_\mu}{2M}, \\ \Gamma'_{4\mu} &= (1 + f_{pp\omega(1420)}) \gamma_\mu - \frac{f_{pp\omega(1420)}(p_2 + p_3)_\mu}{2M}, \end{aligned}$$

where $f_{pp\omega(1420)} = g'_{pp\omega(1420)}/g_{pp\omega(1420)}$.

Hence, the total amplitude for the $\omega(1420)$ meson exchange is

$$\begin{aligned}
T_{\omega(1420)} &= T_{\omega(1420)}^{direct} + T_{\omega(1420)}^{cross} \\
&= g_{pp\omega(1420)}^2 \frac{F_{\omega(1420)}^2(t)}{t - M_{\omega}^2} [\bar{u}_3(p_3, \lambda_3) \Gamma'_{1\mu} u_1(p_1, \lambda_1)] \\
&\quad \times [\bar{u}_4(p_4, \lambda_4) \Gamma_2^{\prime\mu} u_2(p_2, \lambda_2)] \\
&\quad - g_{pp\omega(1420)}^2 \frac{F_{\omega(1420)}^2(u)}{u - M_{\omega}^2} [\bar{u}_4(p_4, \lambda_4) \Gamma'_{3\mu} u_1(p_1, \lambda_1)] \\
&\quad \times [\bar{u}_3(p_3, \lambda_3) \Gamma_4^{\prime\mu} u_2(p_2, \lambda_2)].
\end{aligned} \tag{3.41}$$

So far we have derived all the amplitudes for each exchanged particle. The total amplitude we need is just the sum of all the individual amplitudes,

$$T = T_{\gamma} + T_{\pi} + T_{\rho} + T_{\omega} + T_{\sigma} + T_{f_2} + T_{\omega(1420)}, \tag{3.42}$$

which can be pictorially represented as in Fig.3.4. This is the amplitude we need in constructing the differential cross section. By calculating the five terms T_1, T_2, T_3, T_4 , and T_5 mentioned in the previous section, the differential cross section for the proton-proton elastic scattering can be obtained from (3.10) or (3.11).

Listed here are all the free parameters for the total amplitude

- (i) For π meson : $g_{pp\pi}^2/4\pi, \Lambda_{\pi}$
- (ii) For ρ meson : $g_{pp\rho}^2/4\pi, \Lambda_{\rho}$, and $f_{pp\rho}$
- (iii) For ω meson : $g_{pp\omega}^2/4\pi, \Lambda_{\omega}$
- (iv) For σ meson : $g_{pp\sigma}^2/4\pi, \Lambda_{\sigma}$
- (v) For f_2 meson : $g_{ppf_2}^2/4\pi, \Lambda_{f_2}$, and f_{ppf_2}
- (vi) For $\omega(1420)$ meson : $g_{pp\omega(1420)}^2/4\pi, \Lambda_{\omega(1420)}$, and $f_{pp\omega(1420)}$

which are the coupling constant, the cutoff parameter, and the ratio of the coupling constants, respectively. The next step is to fit these free parameters from the theoretical consistency with the experimental data, which will be discussed in the next chapter.

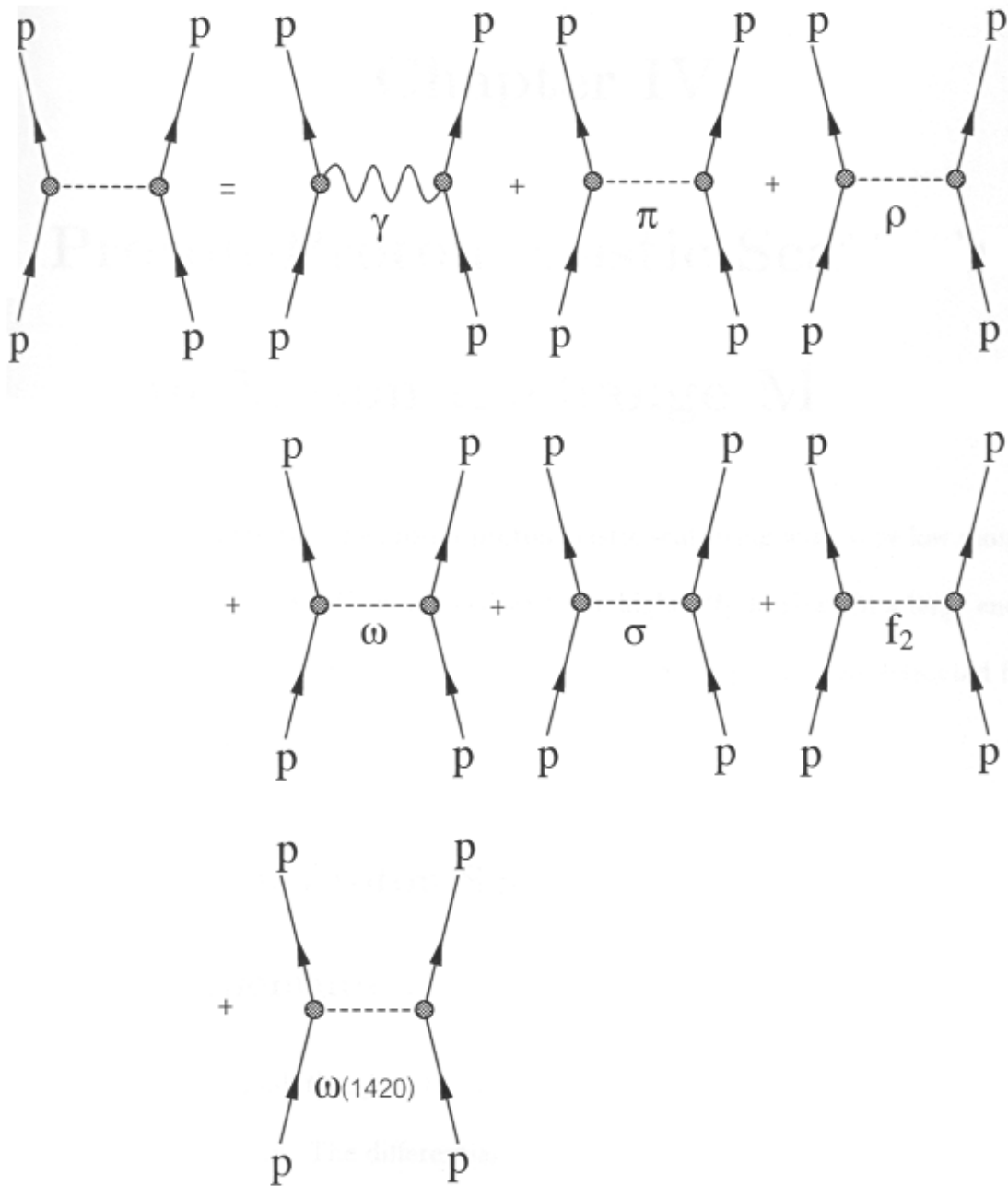


Figure 3.4 The pictorial representing the contribution to the total amplitude from each particle exchange amplitude.

Chapter IV

Proton-Proton Elastic Scattering in Meson Exchange Model

We consider first the proton-proton elastic scattering with very low momentum transfer (small $|t|$), then proceed with the higher $|t|$ involved in a large energy region, $s = 552.3$ to 3906.3 GeV². Finally, the radii of proton are extracted from the theoretical predictions.

4.1 Proton-Proton Scattering with Small Momentum Transfer

For very small $|t|$ region, the $d\sigma/dt$ is known to be dominated by the electromagnetic interaction. The differential cross section for the one- γ exchange process can be easily derived as follows:

$$\begin{aligned} \frac{d\sigma^{(\gamma)}}{dt} &= \frac{\alpha^2 F_1^4(t)}{16st^2} \frac{4\pi}{s - 4M^2} Tr\{\Gamma_{1\mu}(\gamma \cdot p_3 + M)\Gamma_{1\nu}(\gamma \cdot p_1 + M)\} \\ &\quad \times Tr\{\Gamma^{1\mu}(\gamma \cdot p_4 + M)\Gamma^{1\nu}(\gamma \cdot p_2 + M)\} \end{aligned}$$

$$\begin{aligned}
\frac{d\sigma^{(\gamma)}}{dt} &= \frac{\alpha^2 F_1^4(t)}{16st^2} \frac{4\pi}{s - 4M^2} (64M^4 - 64M^2s + 16s^2 + 64f_{pp\gamma}M^2t + 16st \\
&\quad + 32f_{pp\gamma}^2st - \frac{8f_{pp\gamma}^2s^2t}{M^2} + 8t^2 + 32f_{pp\gamma}t^2 + 72f_{pp\gamma}^2t^2 + 32f_{pp\gamma}^3t^2 + 8f_{pp\gamma}^4t^2 \\
&\quad - \frac{8f_{pp\gamma}^2st^2}{M^2} - \frac{4f_{pp\gamma}^4st^2}{M^2} + \frac{f_{pp\gamma}^4s^2t^2}{M^4} + \frac{4f_{pp\gamma}^3t^3}{M^2} + \frac{f_{pp\gamma}^4st^3}{M^4} + \frac{f_{pp\gamma}^4t^4}{4M^4}) \\
&\approx \frac{4\pi\alpha^2 G_E^4(t)}{t^2}, \tag{4.1}
\end{aligned}$$

where $\alpha \equiv e^2/4\pi$. $\Gamma_{1\mu}$ and $\Gamma_{2\mu}$ are defined by

$$\begin{aligned}
\Gamma_{1\mu} &= (1 + f_{pp\gamma})\gamma_\mu - \frac{f_{pp\gamma}(p_1 + p_3)_\mu}{2M}, \\
\Gamma_{2\mu} &= (1 + f_{pp\gamma})\gamma_\mu - \frac{f_{pp\gamma}(p_2 + p_4)_\mu}{2M},
\end{aligned}$$

where $f_{pp\gamma} = 1.79$ (see also section 3.3.1). Note that, for small $|t|$, $F_1(t) \approx G_E(t)$. Shown as dashed lines in Fig. 4.1 are the contributions of the one- γ exchange to the differential cross section of the high energy proton-proton elastic scattering at energies $s = 552.3$ and 942.5 GeV². It is found that the contribution of the electromagnetic interaction drops rapidly as $|t|$ increases. The theoretical prediction is only about 1% of the experimental data for $|t| = 0.01$ (GeV/c)², and about 0.1% for $|t| = 0.05$ (GeV/c)². It is clear that one has to include the strong interaction for the high energy proton-proton elastic scattering even with very low momentum transfers. The momentum transfer involved is so low that the meson cloud (quark sea) interaction should dominate the strong interaction. It is reasonable to assume that only the lightest mesons, the pseudoscalar meson $\pi(140)$, the vector mesons $\rho(770)$ and $\omega(780)$, and the scalar meson $\sigma(980)$ are mainly responsible for the strong interaction at small $|t|$ region. Let us study the differential cross sections due to the exchange of these mesons. We need to consider here only the direct process since the contribution of the cross diagram is largely suppressed for small $|t|$.

For the π exchange, the differential cross section is derived as

$$\begin{aligned}
\frac{d\sigma^{(\pi)}}{dt} &= \frac{G_{pp\pi}^4 F^4(t)}{16s(t-m_\pi^2)^2} \frac{4\pi}{s-4M^2} \text{Tr}\{\Gamma_1(\gamma \cdot p_1 + M)\Gamma_1(\gamma \cdot p_3 + M)\} \\
&\quad \times \text{Tr}\{\Gamma_2(\gamma \cdot p_2 + M)\Gamma_2(\gamma \cdot p_4 + M)\} \\
&= \frac{16\pi G_{pp\pi}^4 M^4 t^2}{s(s-4M^2)(t-m_\pi^2)^2} \\
&\approx \frac{16\pi G_{pp\pi}^4 M^4 t^2}{s^2 m_\pi^4}, \tag{4.2}
\end{aligned}$$

where $G_{pp\pi} \equiv g_{pp\pi}/\sqrt{4\pi}$ is the coupling constant and $F(t)$ is the form factor. For very small $|t|$, $F(t) \approx 1$. Note that, in the derivation of the above expression we have used

$$\begin{aligned}
\Gamma_1 &= \gamma_5 \gamma_\mu (p_1 - p_3)^\mu, \\
\Gamma_2 &= \gamma_5 \gamma_\mu (p_2 - p_4)^\mu,
\end{aligned}$$

and the approximation that $s \gg 4M^2$ and $|t| \ll 1$. It is found in (4.2) that the pion-exchange contribution is very small for low $|t|$.

For the ω exchange, the differential cross section is

$$\begin{aligned}
\frac{d\sigma^{(\omega)}}{dt} &= \frac{G_{pp\omega}^4 F^4(t)}{16s(t-m_\omega^2)^2} \frac{4\pi}{s-4M^2} \text{Tr}\{\gamma_\mu(\gamma \cdot p_1 + M)\gamma_\nu(\gamma \cdot p_3 + M)\} \\
&\quad \times \text{Tr}\{\gamma^\mu(\gamma \cdot p_2 + M)\gamma^\nu(\gamma \cdot p_4 + M)\} \\
&= \frac{4\pi G_{pp\omega}^4}{16s(s-4M^2)(t-m_\omega^2)^2} (64M^4 - 64M^2s + 16s^2 + 16st + st^2) \\
&\approx \frac{4\pi G_{pp\omega}^4}{m_\omega^4}. \tag{4.3}
\end{aligned}$$

Notice that the ω exchange gives rise to a constant contribution to the pp differential cross section $d\sigma/dt$.

For the ρ exchange, we have

$$\begin{aligned}
\frac{d\sigma^{(\rho)}}{dt} &= \frac{G_{pp\rho}^4 F^4(t)}{16s(t-m_\rho^2)^2} \frac{4\pi}{s-4M^2} \text{Tr}\{\bar{\Gamma}_{1\mu}(\gamma \cdot p_3 + M)\bar{\Gamma}_{1\nu}(\gamma \cdot p_1 + M)\} \\
&\quad \times \text{Tr}\{\bar{\Gamma}^{1\mu}(\gamma \cdot p_4 + M)\bar{\Gamma}^{1\nu}(\gamma \cdot p_2 + M)\} \\
&= \frac{G_{pp\rho}^4 F^4(t)}{16s(t-m_\rho^2)^2} \frac{4\pi}{s-4M^2} (64M^4 - 64M^2s + 16s^2 + 64f_{pp\rho}M^2t + 16st \\
&\quad + 32f_{pp\rho}^2st - \frac{8f_{pp\rho}^2s^2t}{M^2} + 8t^2 + 32f_{pp\rho}t^2 + 72f_{pp\rho}^2t^2 + 32f_{pp\rho}^3t^2 + 8f_{pp\rho}^4t^2 \\
&\quad - \frac{8f_{pp\rho}^2st^2}{M^2} - \frac{4f_{pp\rho}^4st^2}{M^2} + \frac{f_{pp\rho}^4s^2t^2}{M^4} + \frac{4f_{pp\rho}^3t^3}{M^2} + \frac{f_{pp\rho}^4st^3}{M^4} + \frac{f_{pp\rho}^4t^4}{4M^4}) \\
&\approx \frac{4\pi G_{pp\rho}^4}{m_\rho^4}, \tag{4.4}
\end{aligned}$$

where we have used

$$\begin{aligned}
\bar{\Gamma}_{1\mu} &= (1 + f_{pp\rho})\gamma_\mu - \frac{f_{pp\rho}(p_1 + p_3)_\mu}{2M}, \\
\bar{\Gamma}_{2\mu} &= (1 + f_{pp\rho})\gamma_\mu - \frac{f_{pp\rho}(p_2 + p_4)_\mu}{2M}.
\end{aligned}$$

Just as expected, the ρ contribution is similar to that of the ω exchange.

For the σ exchange, we have

$$\begin{aligned}
\frac{d\sigma^{(\sigma)}}{dt} &= \frac{G_{pp\sigma}^4 F^4(t)}{16s(t-m_\sigma^2)^2} \frac{4\pi}{s-4M^2} \text{Tr}\{(\gamma \cdot p_1 + M)(\gamma \cdot p_3 + M)\} \\
&\quad \times \text{Tr}\{(\gamma \cdot p_4 + M)(\gamma \cdot p_2 + M)\} \\
&= \frac{G_{pp\sigma}^4 F^4(t)}{16s(t-m_\sigma^2)^2} \frac{4\pi}{s-4M^2} (4M^2 - t)^2 \\
&\approx \frac{4\pi G_{pp\sigma}^4 M^4}{s^2 m_\sigma^4}. \tag{4.5}
\end{aligned}$$

It is obvious that for small $|t|$ and high energies, the σ contribution is negligible.

As the π and σ contributions are ruled out, the vector-meson-exchange contributions, which are approximately constants as shown above, must be significant for small momentum transfer. However, a study of the high energy neutron-proton scattering reveals that the coupling constant of the $NN\rho$ is much smaller than that

of the $NN\omega$ system. (Yan and Tegen, 2000) Therefore, one may conclude that, in addition to the γ exchange, the ω exchange is the only significant process for the high energy pp scattering at low momentum transfers. Shown as solid lines in Fig. 4.1 are the theoretical predictions to the pp scattering. $d\sigma/dt$ in the model includes both the γ and ω exchanges with the coupling constant of $NN\omega$ taking the value

$$\frac{g_{pp\omega}^2}{4\pi} = 2.35 \quad (4.6)$$

In the model, we just let the $NN\omega$ form factor to be 1 and the coupling constant of $NN\omega$ fitted to the experimental data.

It is found in Fig.4.1 that the experimental data are well reproduced for low momentum transfers except for the region from $|t| \approx 0.001$ $(\text{GeV}/c)^2$ to $|t| \approx 0.02$ $(\text{GeV}/c)^2$. That is, the Coulomb interaction region and the strong interaction region for small $|t|$ are well understood in the simple model ($\gamma + \omega$ exchanges). The theoretical prediction for the pp differential cross section at the Coulomb-strong interference region is not in a good agreement with the experimental data. It might be necessary to employ higher-order diagrams to understand the pp differential cross section in the electromagnetic-strong interference region.

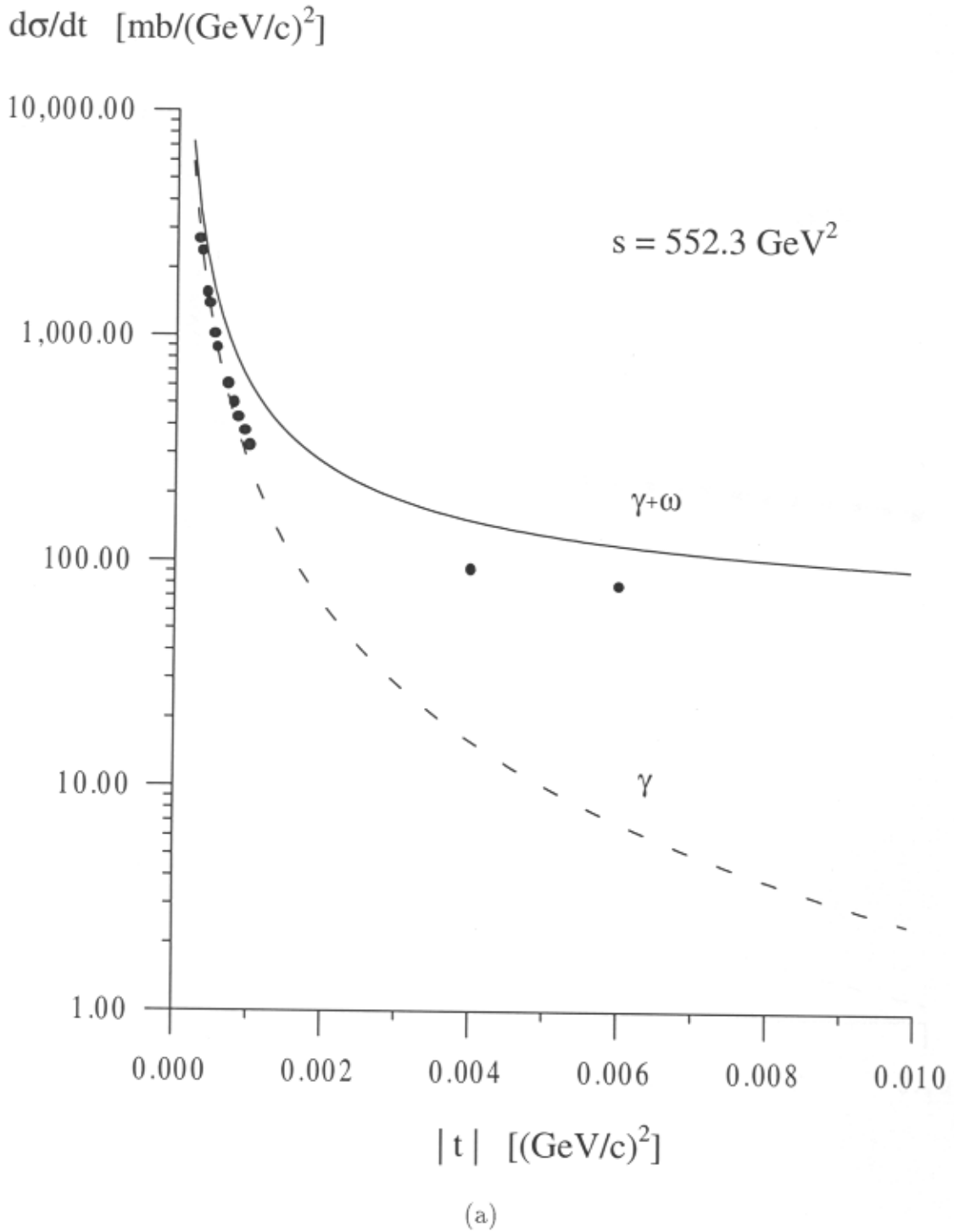
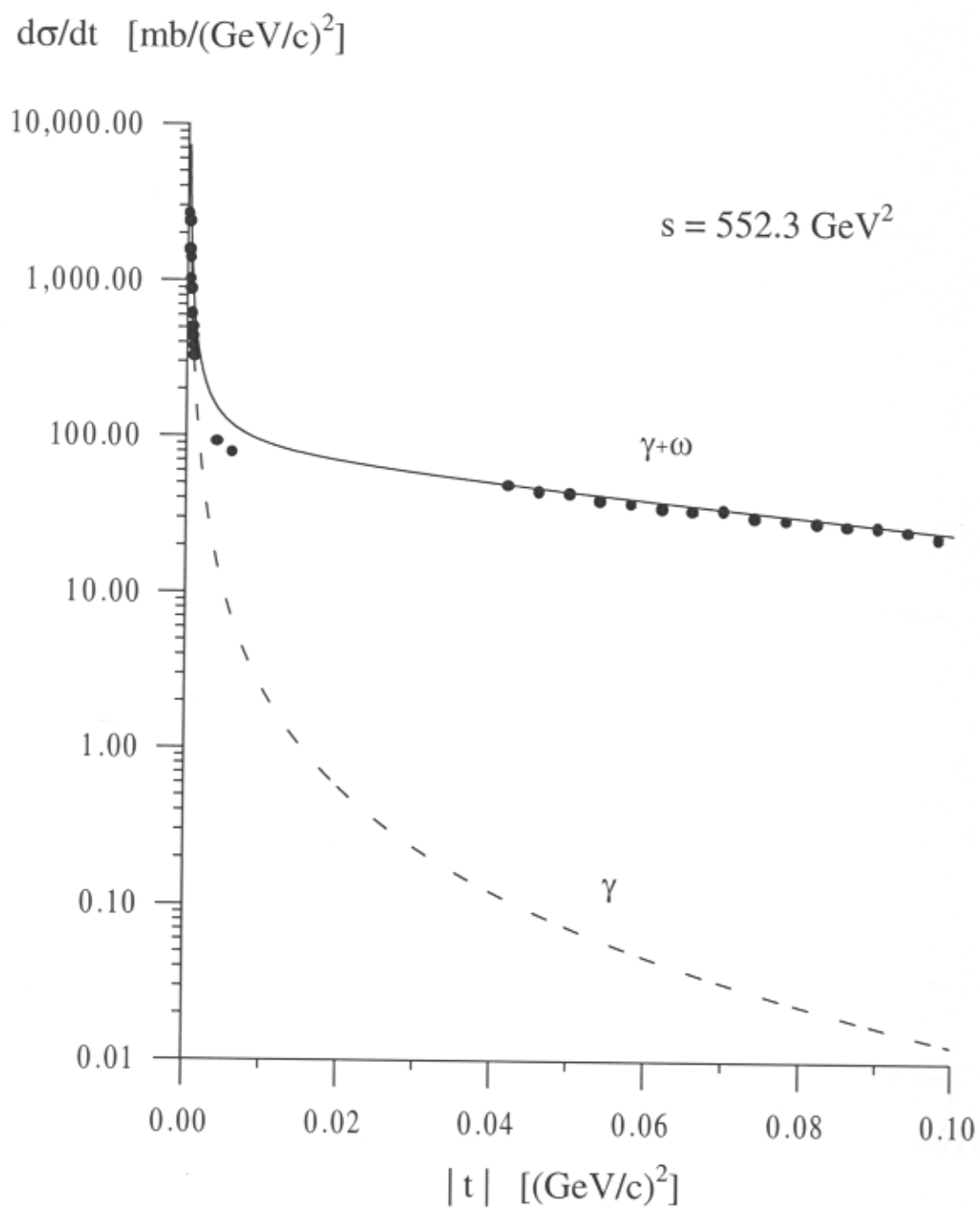


Figure 4.1 The $d\sigma/dt$ due to the γ exchange and the $\gamma + \omega$ exchange for (a) $|t| < 0.01(\text{GeV}/c)^2$, $s = 552.3 \text{ GeV}^2$, (b) $|t| < 0.1(\text{GeV}/c)^2$, $s = 552.3 \text{ GeV}^2$, (c) $|t| < 0.01(\text{GeV}/c)^2$, $s = 942.5 \text{ GeV}^2$, and (d) $|t| < 0.1(\text{GeV}/c)^2$, $s = 942.5 \text{ GeV}^2$.

Data are taken from Schopper (ed.), 1980, pp. 269-276.



(b)

Figure 4.1 (continued)

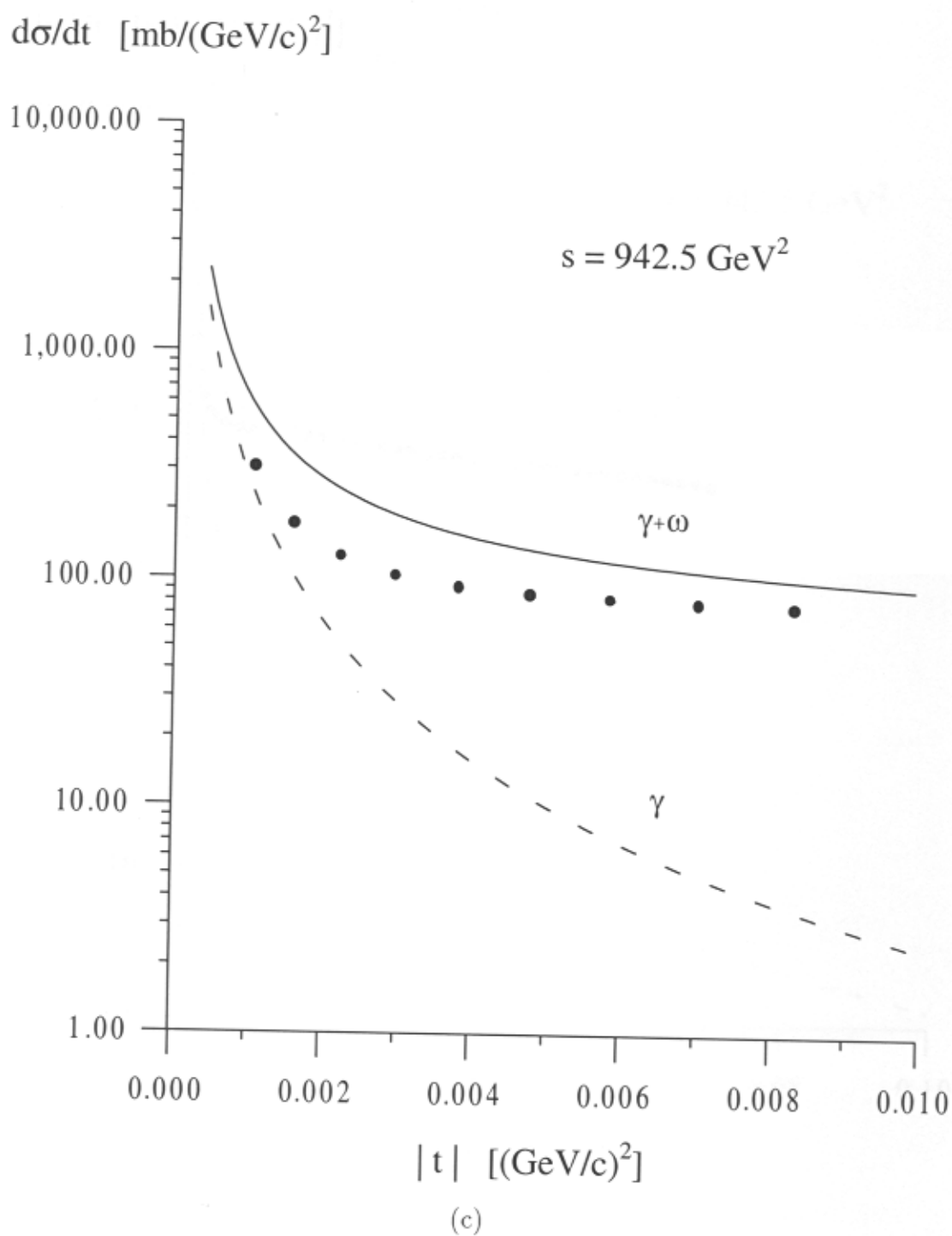
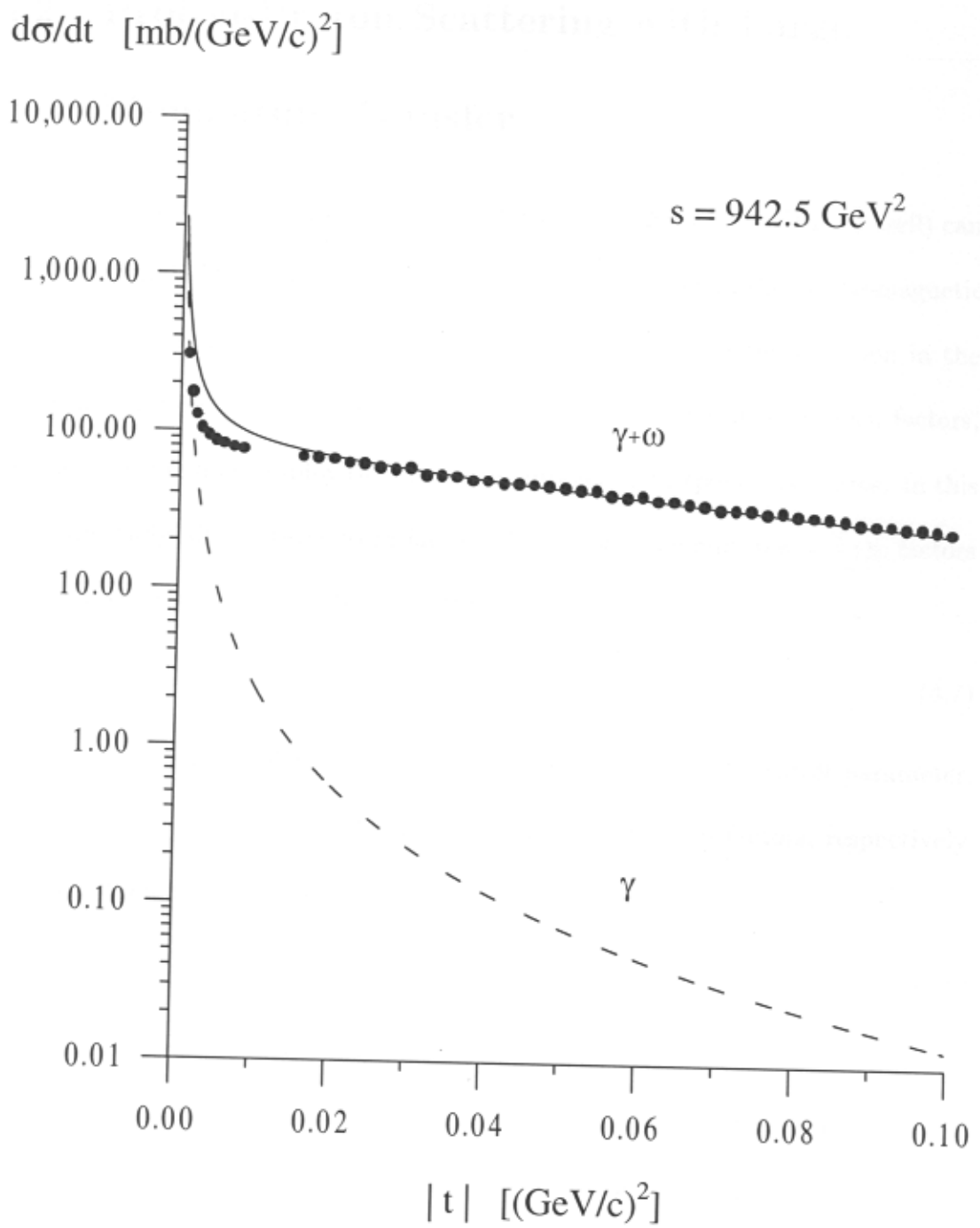


Figure 4.1 (continued)



(d)

Figure 4.1 (continued)

4.2 Proton-Proton Scattering with Large Momentum Transfer

For large momentum transfer, the form factor $F(t)$ (and $F(u)$ as well) can not approximated to be 1 as in the previous section. Unlike in the electromagnetic interaction, the problem of nucleon form factors is still an open question in the strong interaction. There are many possible choices for the nucleon form factors, for example, one may employ the monopole, dipole, and exponential forms. In this work, we study all the three form factors. The monopole and dipole form factors may take the form (Machleidt et al., 1987)

$$F_\alpha(t) = \left(\frac{\Lambda_\alpha^2 - m_\alpha^2}{\Lambda_\alpha^2 - t} \right)^n, \quad (4.7)$$

where m_α is the mass of the exchanged particle, and Λ_α is the cutoff parameter. $n = 1$ and $n = 2$ give rise to the monopole and dipole form factors, respectively. For the exponential form, we use the following form

$$F_\alpha(t) = \exp(t/\Lambda_\alpha^2). \quad (4.8)$$

All of the form factors mentioned above have been employed to fit the experimental data in the theoretical model. It is found that the exponential form is clearly favored by the set of experimental data included in our analysis.

The theoretical fitted curves are presented in Fig. 4.2, where the exponential form factor is employed and the cutoff parameters are set as follows:

$$\Lambda_\pi = \Lambda_\rho = \Lambda_\omega \quad (4.9)$$

and

$$\Lambda_\sigma = \Lambda_{f_2} = \Lambda_{\omega(1420)} \quad (4.10)$$

The best fit to the existing high energy pp elastic data at a large energy range ($s = 552.3$ to $s = 3906.3$ GeV²) gives the following set of coupling constants and size parameters, see Table 4.1.

(4.9) and (4.10) result initially from the consideration that π , ρ and ω belong to the lightest meson group while $\sigma(980)$, $f_2(1270)$ and $\omega(1420)$ are in the second lightest group. The argument in (4.9) and (4.10) is supported by the existing data. If one let all the cutoff parameters independently free in the fitting to the experimental data, it may be found that Λ_π , Λ_ρ and Λ_ω get very close to the values, and so do Λ_σ , Λ_{f_2} and $\Lambda_{\omega(1420)}$.

Table 4.1 The set of parameters best fitted to the experimental data in this work.

Particle	$g^2/4\pi$	Λ [GeV]	f
$\pi(140)$	0.174	0.700	-
$\rho(770)$	0.093	0.700	7.620
$\omega(780)$	2.092	0.700	-
$\sigma(980)$	5.672	1.560	-
$f_2(1270)$	1.654×10^{-5}	1.560	0.078
$\omega(1420)$	0.012	1.560	3.074

Fig. 4.2 show that the experimental data are well reproduced in the present model, which includes only the lowest order Feynman diagrams for γ and meson exchanges without the quark-gluon interaction involved. It is found that for lower $|t|$ region ($|t| < 1.5$ (GeV/c)²) π , ρ and ω are the main contributors while the heavier mesons $\sigma(980)$, $f_2(1270)$ and $\omega(1420)$ play an important role for higher $|t|$

($|t| > 1.5 \text{ (GeV/c)}^2$). Without these heavier mesons, it is impossible to reproduce the large $|t|$ data. The dip-structure at $|t| \approx 1.5 \text{ (GeV/c)}^2$ for all the energies involved here results from the destructive interference between the contributions of the two meson groups.

4.3 Proton Size

The size of proton could be extracted from form factors since a form factor is just the momentum-space representation of a coordinate space distribution. One can easily derive the proton size parameter (mean-square-radius) using the well known expression

$$\langle r^2 \rangle = -6 \left(\frac{dF(\vec{q}^2)}{d\vec{q}^2} \right)_{\vec{q}^2=0}. \quad (4.11)$$

The electromagnetic form factors of nucleon have been confirmed taking the form

$$G(q^2) = \frac{1}{(1 + \vec{q}^2/\Lambda^2)^2}, \quad (4.12)$$

with $\Lambda^2 = 0.71 \text{ GeV}^2$ and the momentum transfer $\vec{q} = \vec{p}_f - \vec{p}_i$, for a large energy region. The form factor corresponds to an exponential distribution in coordinate space

$$\rho(r) = \rho_0 e^{-\Lambda r} \quad (4.13)$$

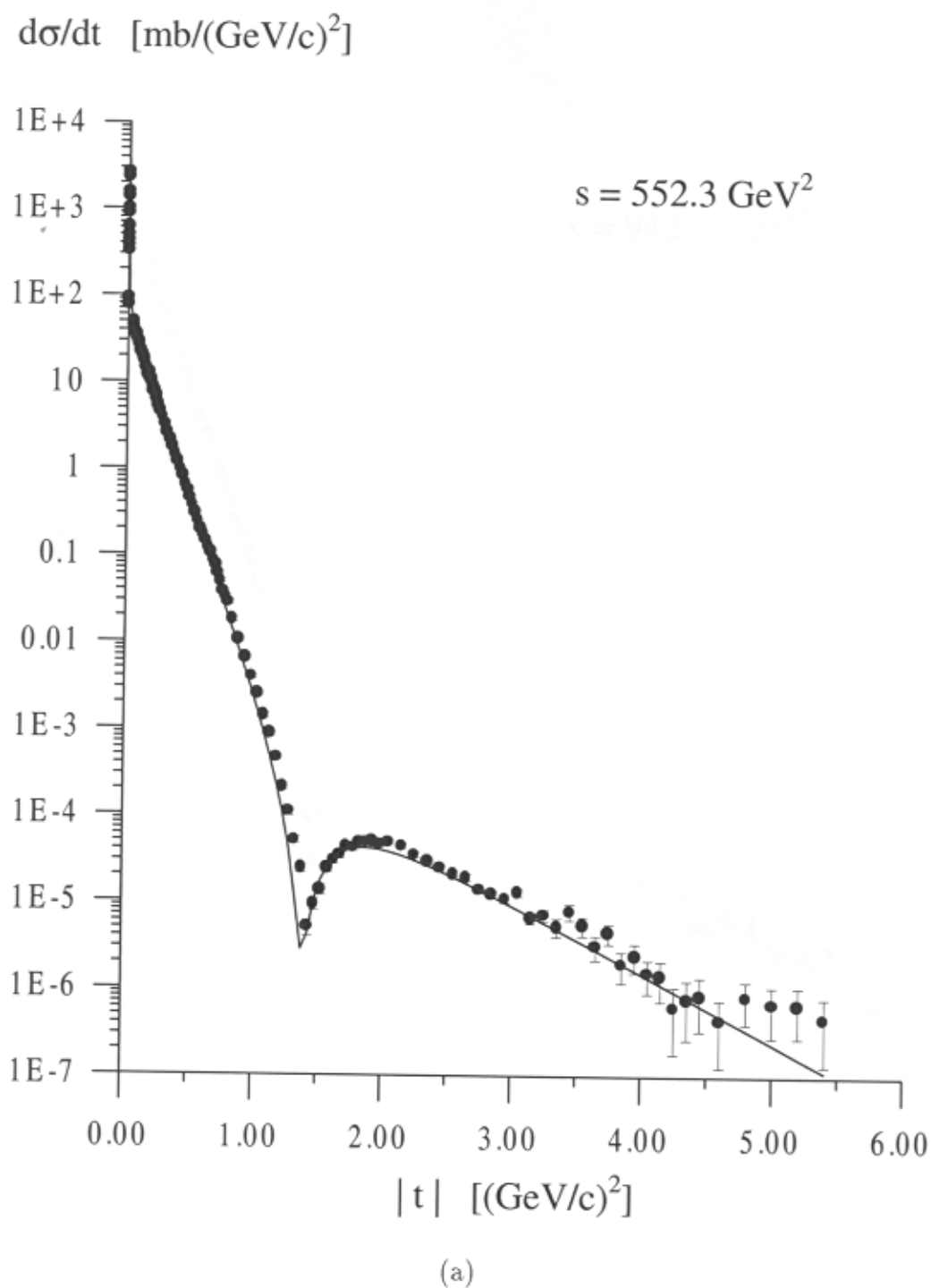
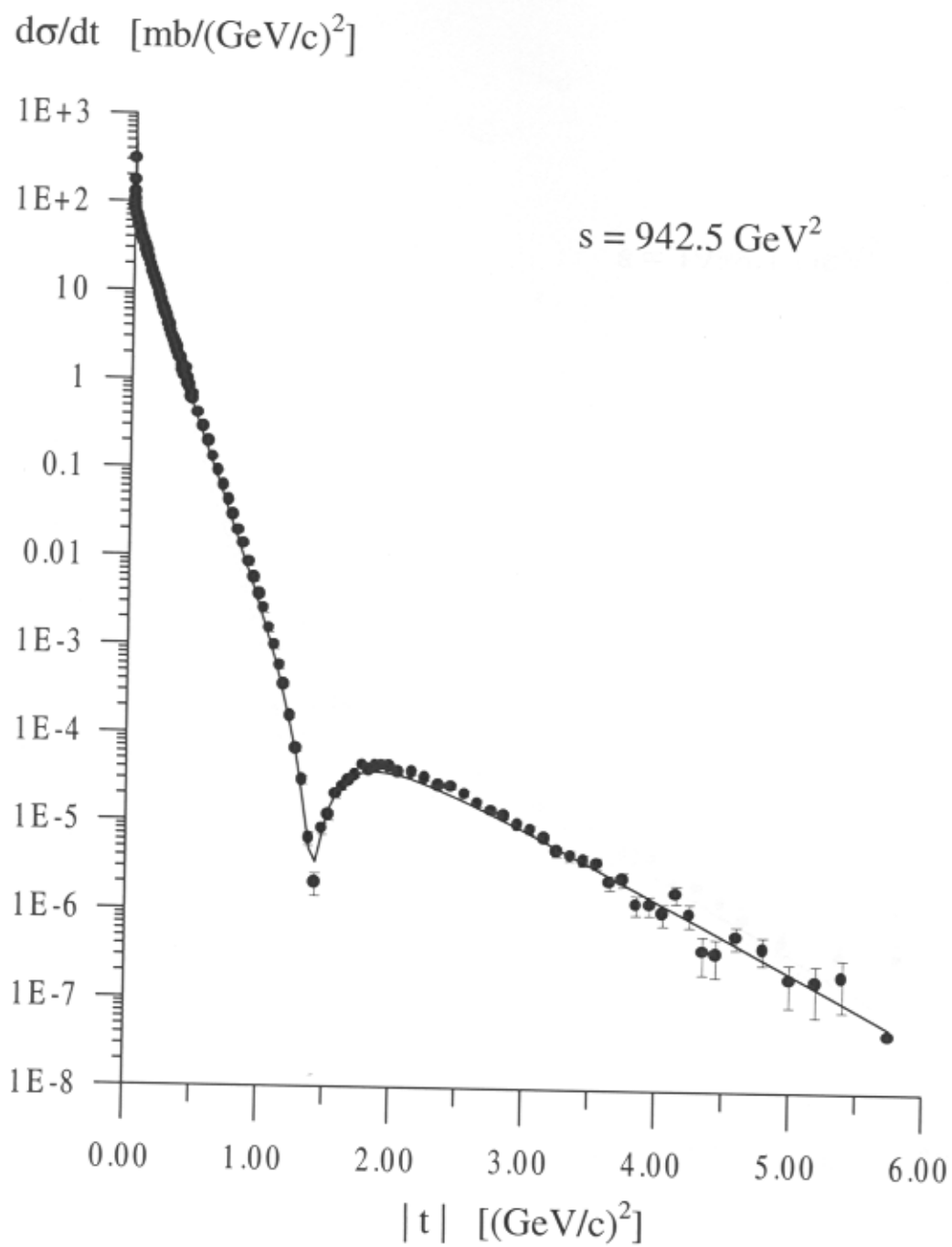
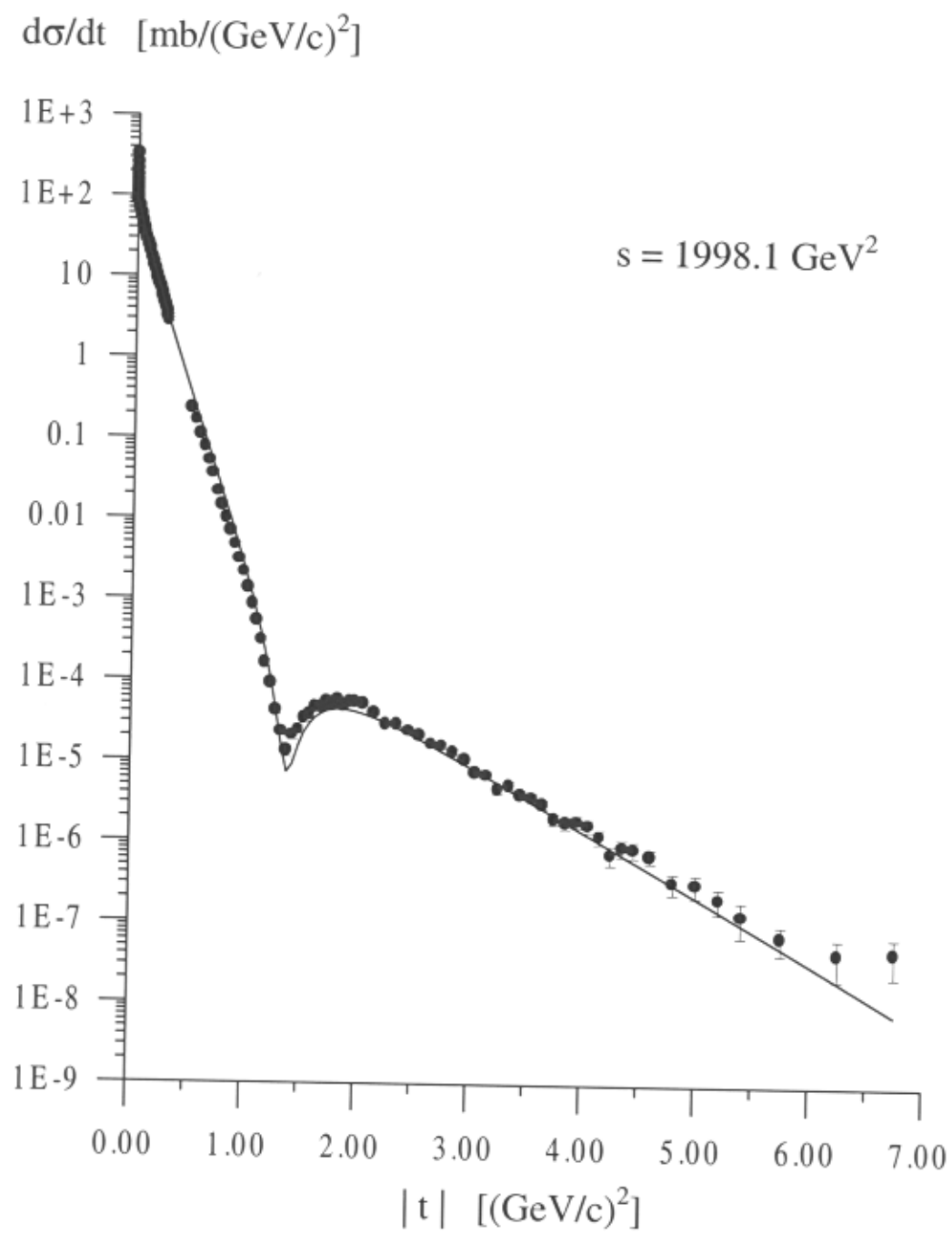


Figure 4.2 The $d\sigma/dt$ in the one-body-exchange model (solid line) versus the experimental data for (a) $s = 552.3 \text{ GeV}^2$, (b) $s = 942.5 \text{ GeV}^2$, (c) $s = 1998.1 \text{ GeV}^2$, (d) $s = 2787.8 \text{ GeV}^2$, and (e) $s = 3906.3 \text{ GeV}^2$. Data are taken from Schopper (ed.), 1980, pp. 269-286.



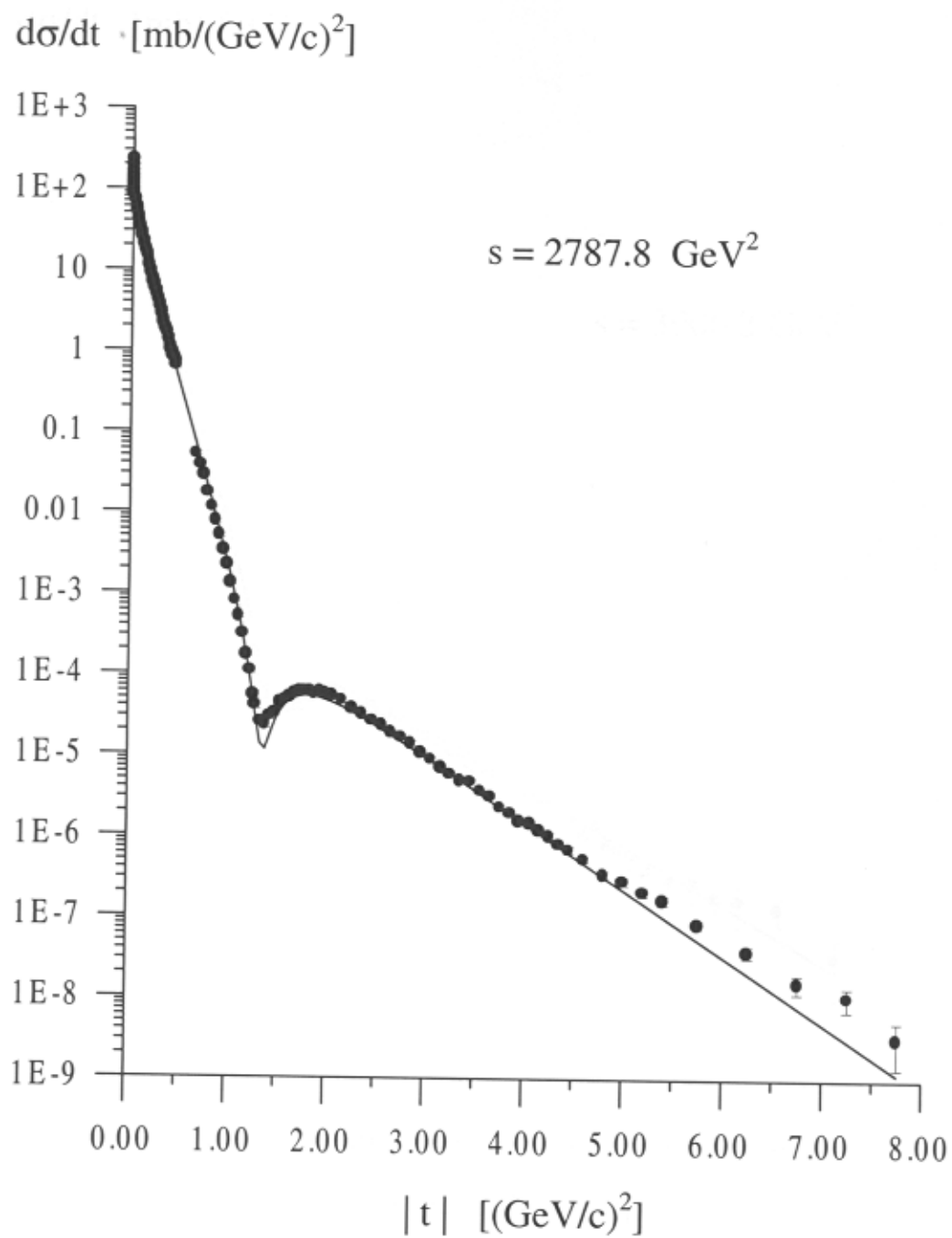
(b)

Figure 4.2 (continued)



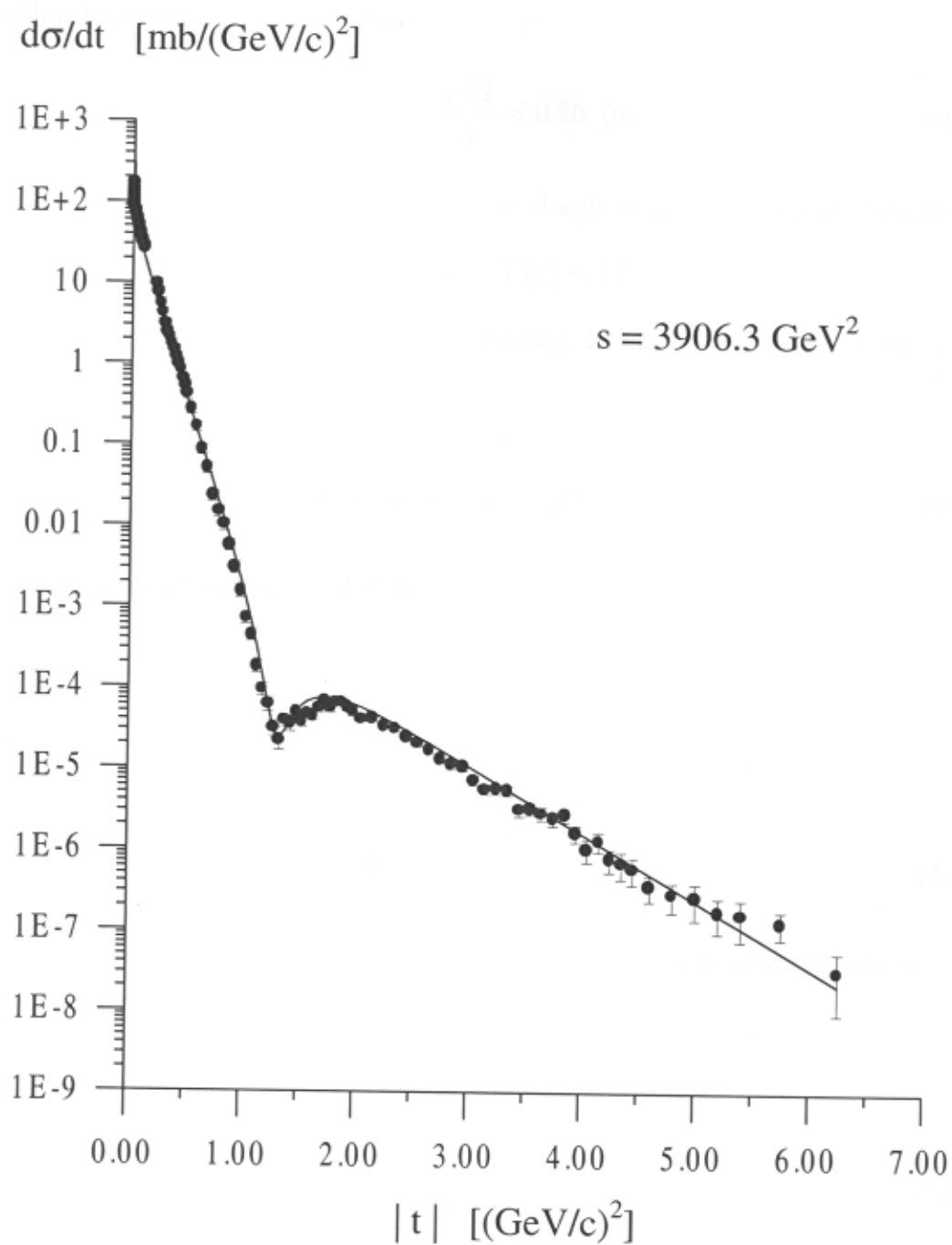
(c)

Figure 4.2 (continued)



(d)

Figure 4.2 (continued)



(e)

Figure 4.2 (continued)

with a root-mean-square radius

$$\langle r^2 \rangle^{1/2} = \frac{\sqrt{12}}{\Lambda} \approx 0.80 \text{ fm.} \quad (4.14)$$

The form in (4.13) seems to reveal that the charge-magnetic-moment distribution stems from the Coulomb-like interaction, $V(r) \sim 1/r$.

We come to the proton-proton scattering. In the center-of-mass system, one has

$$t = -\vec{q}^2 = -(\vec{p}_f - \vec{p}_i)^2. \quad (4.15)$$

Thus the vertex function in (4.8) is

$$F(t) = F(\vec{q}^2) = e^{-\vec{q}^2/\Lambda^2}, \quad (4.16)$$

which corresponds to a distribution in coordinate space as follows

$$\rho(r) = \rho_0 e^{-\Lambda^2 r^2}. \quad (4.17)$$

An interaction of the form $V(r) \sim r^2$ could lead to this type of distributions.

The cutoff for the π exchange corresponds to a size parameter (see Table 4.1)

$$\langle r^2 \rangle^{1/2} = \frac{\sqrt{6}}{\Lambda} = \frac{\sqrt{6}}{0.70 \text{ GeV}} \approx 0.69 \text{ fm,} \quad (4.18)$$

while the f_2 exchange corresponds to

$$\begin{aligned} \langle r^2 \rangle^{1/2} &= \frac{\sqrt{6}}{1.56 \text{ GeV}} \\ &\approx 0.31 \text{ fm.} \end{aligned} \quad (4.19)$$

It is difficult to say that the size 0.31 fm does correspond to the quark core since it can also be an inner meson cloud. However, we can surely point out that the size of

the quark core (if any) is smaller than 0.3 fm, and proton is likely to be composed of at least two components: the three-quark core and the quark-antiquark sea surrounding the core.

The quark-antiquark sea itself may have two faces. For the electromagnetic interaction collision it has a distribution of the form $e^{-\Lambda r}$ (from an interaction of Coulomb-like $V(r) \sim 1/r$) with a root-mean-square radius of about 0.8 fm while for the strong interaction collision it has a distribution of the form $e^{-\Lambda^2 r^2}$ (from an interaction of the form $V(r) \sim r^2$) with a root-mean-square radius of about (~ 0.7 fm). The so-called meson cloud might be refer to only the quark-antiquark distribution probed by the strong interaction collision.

The three-quark core has the distribution of the form $e^{-\Lambda^2 r^2}$, which stems from an interaction of the form $V(r) \sim r^2$, with the root-mean-square radius less than 0.3 fm.

Chapter V

Discussion and Conclusion

Here in the last chapter, we give some points to serve as the discussion and conclusion of the work.

5.1 Conclusion

5.1.1 The Model

The model is based on the assumption that proton is composed of at least two components, the quark core and the quark-antiquark sea, and the high energy proton-proton elastic scattering is dominated by the quark sea interaction. The assumption itself stems from the analysis of the existing experimental data. The quark sea interaction is here “parameterized” into meson exchange. In this model, only the lowest order processes are considered with the exchanges of γ for the electromagnetic interaction, and $\pi(140)$, $\rho(770)$, $\omega(780)$, $\sigma(980)$, $f_2(1270)$, and $\omega(1420)$ for the strong interaction. The contribution of quark-gluon interaction is excluded in the model.

5.1.2 Theoretical Differential Cross Section

The theoretical results for the differential cross section of the high energy pp elastic scattering consistently reproduce the existing data in a large

energy region. The most significant features of the experimental data, the dip-structure and the different slopes, are well reproduced in the model. For the lower $|t|$ region ($|t| < 1.5 \text{ (GeV/c)}^2$) the dominant process is the ω exchange while the presence of the heavier mesons f_2 and $\omega(1420)$ is crucial for higher $|t|$ region ($|t| > 1.5 \text{ (GeV/c)}^2$).

5.1.3 Structure of Proton

The analysis of the form factors of proton in Chapter IV reveals that two different components exist within proton. The first component might be the quark core with a size less than 0.3 fm, the second is the quark-antiquark sea which has a size around 0.7 fm probed in the strong interaction collision and a size around 0.8 fm probed in the electromagnetic interaction collision. That the quark core (if any) is smaller than 0.3 fm is in line with the little bag model introduced in Chapter I.

5.2 Comments on the Results

5.2.1 The $\omega(1420)$ Coupling Constant

As shown in (3.39) for the Lagrangian of $NN\omega(1420)$ coupling, there is an additional i involved in the Lagrangian, to prevent the $g_{pp\omega(1420)}^2/4\pi$ from being negative value. It might be the case that the $\omega(1420)$ exchange introduced in this work represents a combined effect. That is, the contribution is not due to the $\omega(1420)$ exchange alone, but due to other meson exchange, multi-meson exchange, and gluon exchange as well as the $\omega(1420)$ exchange.

5.2.2 Coulomb-Strong Interference Region

As mentioned in Chapter IV, the model can not give a satisfactory prediction for the pp differential cross section at the electromagnetic-strong interference region around $|t| = 0.01$ $(\text{GeV}/c)^2$. The momentum transfer involved is so small that the direct quark core interaction is not expected. It is likely that the higher-order diagrams, for example, the two-photon-exchange process should be added to the processes in Fig. 3.4 for constructing the total amplitude.

References

- Brodsky, S. J., Carlson, C. E., and Lipkin, H. (1979). Spin effects in large-transverse-momentum exclusive scattering processes. **Phys. Rev. D.** 20 (9) : 2278-2289.
- Brown, G. E., and Rho, M. (1979). The little bag. **Phys. Lett. B** 82 (2) : 177-180.
- Chodos, A., Jaffe, R. L., Johnson, K., Thorn, C. B., and Weisskopf, V. F. (1974). New extended model of hadrons. **Phys. Rev. D.** 9 (12) : 3471-3495.
- Cottingham, W. N., Lacombe, M., Loiseau, B., Richard, J. M., and Mau, R. V. (1973). Nucleon-nucleon interaction from pion-nucleon phase-shift analysis. **Phys. Rev. D.** 8 (3) : 800-819.
- Farrar, G. R., Gottlieb, S., Sivers, D., and Thomas, G. H. (1979). Constituent description of NN elastic scattering observables at large angles. **Phys. Rev. D.** 20 (1) : 202-210.
- Gibbs, W. R., and Loiseau, B. (1994). Neutron-proton charge exchange. **Phys. Rev. C.** 50 (6) : 2742-2755.
- Griffiths, D.J. (1987). **Introduction to elementary particle.** Singapore : John Wiley & Sons.
- Halzen, F., Martin, A. D. (1984). **Quarks and Leptons.** New York : John Wiley & Sons.
- Hansen, P. H., and Krisch, A. D. (1977). Universal fit to p-p elastic diffraction scattering from the Lorentz-contracted geometrical model. **Phys. Rev.**

- Phys. Rev. **D.** 15 (11) : 3287-3295.
- Kaku, M. (1993). **Quantum field theory : a modern introduction.**
New York : Oxford University Press.
- Landshoff, P. V. (1974). Model for elastic scattering at wide angle. **Phys. Rev.**
D. 10 (3) : 1024-1030.
- Machleidt, R., Holinde, K., and Elster, Ch. (1987). The Bonn meson-exchange
model for the nucleon-nucleon interaction. **Phys. Rep.** 149 (1) : 1-89.
- Nath, L.M. (1965). The minimal electromagnetic interactions of the charged spin
2 field. **Nucl. Phys.** 68 : 660-672.
- Particle Data Group. (1998). Review of particle physics. **Eur. Phys. J. C.** 3
(1-4) : 1-794.
- Ryder, L. H. (1994). **Quantum field theory.** Newcastle, England : Cambridge
University Press.
- Schopper, H. (ed.) (1980). **Landolt-Brönstein, New Series, Group I.** Vol.9a.
Berlin : Springer-Verlag.
- Serber, R. (1963). Theory of scattering with large momentum transfer. **Phys.Rev.**
Lett. 10 (8) : 357-360.
- Stone, J.L., Chanowski, J.P., Gray, S.W., Gustafson, H.R., Jones, L.W., Longo,
M.J. (1977). Large-Angle neutron-proton elastic scattering from 5 to 12
GeV/c. **Phys. Rev. Lett.** 38 : 1315-1317.
- Thomas, A. W., Thèberge, S., and Miller, G. A. (1981). Cloudy bag model of the
nucleon. **Phys. Rev. D.** 24 (1) : 216-229.
- Yan, Y., and Tegen, R. (1996). Role of tensor meson pole and Δ exchange diagrams
in $p\bar{p} \rightarrow \pi^+\pi^-$. **Phys. Rev. C.** 54 (3) : 1441-1450.

Yan, Y., and Tegen, R. (2000). *pn* charge exchange scattering. (to be submitted)

Appendix A

The Mandelstam Variables

For the scattering process

$$1 + 2 \rightarrow 3 + 4, \quad (\text{A.1})$$

the Mandelstam variables are defined by

$$s = (p_1 + p_2)^2, \quad (\text{A.2})$$

$$t = (p_3 - p_1)^2, \quad (\text{A.3})$$

$$u = (p_4 - p_1)^2, \quad (\text{A.4})$$

where p_i is the energy-momentum four vector. The three variables are not independent, but obey a relation that

$$\begin{aligned} s + t + u &= (p_1 + p_2)^2 + (p_3 - p_1)^2 + (p_4 - p_1)^2 \\ &= (p_1^2 + 2p_1 \cdot p_2 + p_2^2) + (p_3^2 - 2p_1 \cdot p_3 + p_1^2) + (p_4^2 - 2p_1 \cdot p_4 + p_1^2) \\ &= 3p_1^2 + p_2^2 + p_3^2 + p_4^2 + 2(p_1 \cdot p_2 - p_1 \cdot p_3 - p_1 \cdot p_4) \\ &= 3p_1^2 + p_2^2 + p_3^2 + p_4^2 + 2p_1 \cdot (p_2 - p_3 - p_4) \\ &= 3p_1^2 + p_2^2 + p_3^2 + p_4^2 - 2p_1^2 \\ &= p_1^2 + p_2^2 + p_3^2 + p_4^2 \\ &= m_1^2 + m_2^2 + m_3^2 + m_4^2. \end{aligned}$$

That is

$$s + t + u = \sum_{i=1}^4 m_i^2. \quad (\text{A.5})$$

In the center-of-mass system (denoted as CM from now on) as shown in Fig. 3.2, for the elastic scattering process of two equal-mass particles, we may write s , t , and u in the explicit form as follows:

$$\begin{aligned} s &= (p_1 + p_2)^2 \\ &= (E_1 + E_2)^2 - (\vec{p}_1 + \vec{p}_2)^2 \\ &= (2E)^2 \\ &= E_{cm}^2, \end{aligned} \quad (\text{A.6})$$

where E_{cm} is the total energy in the CM system, and E the energy of each particle as

$$E = \sqrt{\vec{p}^2 + m^2}. \quad (\text{A.7})$$

For the other Mandelstam variables t and u , we have

$$\begin{aligned} t &= (p_3 - p_1)^2 \\ &= (E_3 - E_1)^2 - (\vec{p}_3 - \vec{p}_1)^2 \\ &= -(\vec{p}_3^2 + \vec{p}_1^2 - 2\vec{p}_1 \cdot \vec{p}_3) \\ &= -2p^2(1 - \cos\theta), \end{aligned} \quad (\text{A.8})$$

$$\begin{aligned} u &= (p_4 - p_1)^2 \\ &= (E_4 - E_1)^2 - (\vec{p}_4 - \vec{p}_1)^2 \\ &= -(\vec{p}_4^2 + \vec{p}_1^2 - 2\vec{p}_1 \cdot \vec{p}_4) \\ &= -2p^2(1 + \cos\theta). \end{aligned} \quad (\text{A.9})$$

Appendix B

The Dirac Spinor

The *free* spin- $\frac{1}{2}$ particle satisfies the free Dirac equation

$$(i\gamma^\mu\partial_\mu - m)\psi = 0, \quad (\text{B.1})$$

where μ is running from 1 to 4 and the γ^μ are the 4×4 matrices with the properties

$$(\gamma^0)^2 = 1$$

$$(\gamma^i)^2 = -1 \text{ where } i = 1, 2, 3$$

$$\gamma^\mu\gamma^\nu + \gamma^\nu\gamma^\mu = 0 \text{ for } \mu \neq \nu$$

We can summarize the above set of equations to be

$$\{\gamma^\mu, \gamma^\nu\} = 2g^{\mu\nu}, \quad (\text{B.2})$$

where $g^{\mu\nu}$ is the element of the matrix g defined as

$$g = \begin{pmatrix} 1 & 0 & 0 & 0 \\ 0 & -1 & 0 & 0 \\ 0 & 0 & -1 & 0 \\ 0 & 0 & 0 & -1 \end{pmatrix}. \quad (\text{B.3})$$

The explicit representation of the γ^μ matrices is not unique. In this work we use one of the two most popular forms listed, see below:

$$\gamma^0 = \begin{pmatrix} I & 0 \\ 0 & -I \end{pmatrix}, \quad (\text{B.4})$$

$$\gamma^i = \begin{pmatrix} 0 & \sigma^i \\ -\sigma^i & 0 \end{pmatrix}, \quad (\text{B.5})$$

where σ^i are the Pauli matrices taking the form

$$\sigma^1 = \begin{pmatrix} 0 & 1 \\ 1 & 0 \end{pmatrix}, \quad (\text{B.6})$$

$$\sigma^2 = \begin{pmatrix} 0 & -i \\ i & 0 \end{pmatrix}, \quad (\text{B.7})$$

$$\sigma^3 = \begin{pmatrix} 1 & 0 \\ 0 & -1 \end{pmatrix}. \quad (\text{B.8})$$

Here below are some useful properties of the γ^μ

$$\gamma^{0\dagger} = \gamma^0, \quad (\text{B.9})$$

$$\gamma^{i\dagger} = -\gamma^i; \quad i = 1, 2, 3. \quad (\text{B.10})$$

From the γ^μ matrices, we may define

$$\gamma^5 \equiv i\gamma^0\gamma^1\gamma^2\gamma^3 \quad (\text{B.11})$$

which has the explicit form

$$\gamma^5 = \begin{pmatrix} 0 & I \\ I & 0 \end{pmatrix}. \quad (\text{B.12})$$

The solutions of the Dirac equation take the general form

$$\psi = Au(p)e^{-ip \cdot x} + Bv(p)e^{ip \cdot x} \quad (\text{B.13})$$

with $u(p)$ and $v(p)$, the Dirac spinors, satisfy the equations

$$\begin{aligned} (\gamma^\mu p_\mu - m)u(p) &= 0, \\ (\gamma^\mu p_\mu + m)v(p) &= 0, \end{aligned} \quad (\text{B.14})$$

which are indeed the Dirac equation in momentum space. By solving the above equations, one may derive the explicit form of the Dirac spinors as follows:

$$u^{(i)}(p) = \sqrt{\frac{E+m}{2m}} \begin{pmatrix} \lambda^i \\ \frac{1}{E+m}(\vec{p} \cdot \vec{\sigma})\lambda^i \end{pmatrix} \quad (\text{B.15})$$

and

$$v^{(i)}(p) = \sqrt{\frac{E+m}{2m}} \begin{pmatrix} \frac{1}{E-m}(\vec{p} \cdot \vec{\sigma})\lambda^i \\ \lambda^i \end{pmatrix} \quad (\text{B.16})$$

where $E = \sqrt{\vec{p}^2 + m^2}$, and λ^i are 2-spinors with $i = 1, 2$. Usually, λ^i are chosen to be the eigenfunctions of the σ^3 or the helicity operators $h = \vec{p} \cdot \vec{\sigma}/|\vec{p}|$. The normalization constant $\sqrt{\frac{E+m}{2m}}$ is chosen so that the Dirac spinors are normalized according to

$$\bar{u}^{(i)}(p)u^{(j)}(p) = \delta_{ij}, \quad (\text{B.17})$$

$$\bar{v}^{(i)}(p)v^{(j)}(p) = -\delta_{ij}, \quad (\text{B.18})$$

where

$$\bar{u} \equiv u^\dagger \gamma^0, \quad (\text{B.19})$$

$$\bar{v} \equiv v^\dagger \gamma^0. \quad (\text{B.20})$$

The completeness relations for the Dirac spinors are

$$\sum_{i=1,2} u^{(i)}(p) \bar{u}^{(i)}(p) = \frac{\gamma \cdot p + m}{2m}, \quad (\text{B.21})$$

$$\sum_{i=1,2} v^{(i)}(p) \bar{v}^{(i)}(p) = \frac{\gamma \cdot p - m}{2m}. \quad (\text{B.22})$$

Appendix C

Differential Cross section

The cross section, $d\sigma$, is represented by

$$d\sigma = \frac{|T|^2}{F} dQ, \quad (\text{C.1})$$

where T is the invariant amplitude, F is the incident flux, and dQ is the Lorentz invariant phase space factor. (see also Halzen, and Martin, 1984, chap.4; Kaku, 1993, chap.5 and chap.6; Ryder, 1994, section 6.10)

First, Let us derive the explicit form of the incident flux F in the CM system for the elastic scattering of two equal-mass particles. The energy of a particle, with the rest mass M moving with the velocity \vec{v} , is (in natural unit, $\hbar = c = 1$)

$$\begin{aligned} E &= \gamma M \\ &= \frac{1}{\sqrt{1 - \vec{v}^2}} M. \end{aligned} \quad (\text{C.2})$$

In term of momentum \vec{p} and rest mass M

$$E = (\vec{p}^2 + M^2)^{1/2} \quad (\text{C.3})$$

Squaring both sides of (C.2) and (C.3), we get

$$\begin{aligned} \frac{1}{1 - \vec{v}^2} M^2 &= \vec{p}^2 + M^2 \\ M^2 &= (1 - \vec{v}^2)(\vec{p}^2 + M^2) \\ \vec{v}^2(\vec{p}^2 + M^2) &= \vec{p}^2 \\ \vec{v}^2 &= \frac{\vec{p}^2}{E^2} \end{aligned} \quad (\text{C.4})$$

or in term of vector

$$\vec{v} = \frac{\vec{p}}{E} \quad (\text{C.5})$$

hence, in the center-of-mass system

$$\begin{aligned} |\vec{v}_1 - \vec{v}_2| &= |\vec{v}_1| + |\vec{v}_2| \\ &= \frac{|\vec{p}_1|}{E_1} + \frac{|\vec{p}_2|}{E_2} \end{aligned} \quad (\text{C.6})$$

Therefore, from the definition of the flux, F ,

$$F = |\vec{v}_1 - \vec{v}_2| \frac{E_1 E_2}{M M}, \quad (\text{C.7})$$

we obtain

$$\begin{aligned} F &= \left(\frac{|\vec{p}_1|}{E_1} + \frac{|\vec{p}_2|}{E_2} \right) \frac{E_1 E_2}{M M} \\ &= \frac{|\vec{p}_1| E_2}{M^2} + \frac{|\vec{p}_2| E_1}{M^2} \\ &= \frac{E_i p}{M^2}, \end{aligned} \quad (\text{C.8})$$

where $E_i = E_1 + E_2 = 2E$ is the initial energy of the two-particle system.

The invariant phase space dQ in the CM system can be written as

$$\begin{aligned} dQ &= (2\pi)^4 \delta^{(4)}(P_f - P_i) \frac{M d^3 p_3}{E_3 (2\pi)^3} \frac{M d^3 p_4}{E_4 (2\pi)^3} \\ &= \frac{1}{(2\pi)^2} \frac{M^2}{E_3 E_4} \delta(E_3 + E_4 - E_1 - E_2) \delta^{(3)}(\vec{p}_3 + \vec{p}_4 - \vec{p}_1 - \vec{p}_2) d^3 p_3 d^3 p_4 \\ &= \frac{1}{(2\pi)^2} \frac{M^2 d^3 p_3}{E_3 E_4} \delta(E_3 + E_4 - E_1 - E_2) \\ &= \frac{1}{(2\pi)^2} \frac{4M^2}{E_f^2} p^2 dp d\Omega \delta(E_f - E_i). \end{aligned} \quad (\text{C.9})$$

From $E_f = E_3 + E_4 = 2(p^2 + M^2)^{1/2}$, one derives

$$\begin{aligned} \frac{dE_f}{dp} &= \frac{2p}{(p^2 + M^2)^{1/2}} \\ &= \frac{4p}{E_f} \end{aligned}$$

or

$$dp = \frac{E_f}{4p} dE_f, \quad (\text{C.10})$$

hence

$$\begin{aligned} dQ &= \frac{1}{(2\pi)^2} \frac{M^2 p dE_f}{E_f} d\Omega \delta(E_f - E_i) \\ &= \frac{1}{(2\pi)^2} \frac{p}{E_i} d\Omega. \end{aligned} \quad (\text{C.11})$$

Finally, from (C.1), (C.8) and (C.11), we get

$$\begin{aligned} d\sigma &= \frac{|T|^2}{F} dQ \\ &= \frac{1}{(2\pi)^2} \frac{M^4}{E_i^2} |T|^2 d\Omega \end{aligned} \quad (\text{C.12})$$

or

$$\frac{d\sigma}{d\Omega} = \frac{1}{(4\pi)^2} \frac{M^4}{E^2} |T|^2. \quad (\text{C.13})$$

For unpolarized scattering, $|T|^2$ should be replaced by

$$|T|^2 \rightarrow \frac{1}{4} \sum_{\lambda_1 \lambda_2 \lambda_3 \lambda_4} |T_{fi}|^2, \quad (\text{C.14})$$

where

$$\begin{aligned} T_{fi} &= \langle f | T | i \rangle \\ &= \langle \lambda_3 \lambda_4 | T | \lambda_1 \lambda_2 \rangle \end{aligned}$$

is the transition amplitude from state i to state f . λ_i is the spin state of the i^{th} particle. Then, (C.13) becomes

$$\frac{d\sigma}{d\Omega} = \frac{1}{(4\pi)^2} \frac{M^4}{E^2} \frac{1}{4} \sum_{\lambda_1 \lambda_2 \lambda_3 \lambda_4} |T_{fi}|^2. \quad (\text{C.15})$$

It is more convenient to use the invariant differential cross section $d\sigma/dt$ in terms of the Mandelstam variables,

$$\frac{d\sigma}{dt} = \frac{d\sigma}{d\Omega} \frac{d\Omega}{dt}, \quad (\text{C.16})$$

where

$$\begin{aligned} \frac{d\Omega}{dt} &= \frac{\sin\theta d\theta d\phi}{dt} \\ &= 2\pi \sin\theta \frac{d\theta}{dt}. \end{aligned} \quad (\text{C.17})$$

From (A.8) in Appendix A, after differentiate t with respect to θ , we have

$$\frac{dt}{d\theta} = -2p^2 \sin\theta. \quad (\text{C.18})$$

Thus, from (C.17) and (C.18), we have

$$\frac{d\Omega}{dt} = -\frac{\pi}{p^2}. \quad (\text{C.19})$$

Since t is always negative, however, we usually plot the differential cross section with respect to $|t|$ (or $-t$) instead of t itself. Conventionally, we just express the differential cross section $d\sigma/dt$ in the form

$$\frac{d\sigma}{dt} = \frac{\pi}{p^2} \frac{d\sigma}{d\Omega} \quad (\text{C.20})$$

with the minus sign ignored.

Appendix D

Vertex Functions for $NN\gamma$, $NN\rho$ and NNf_2 Systems

D.1 Vertex Function for $NN\gamma$ Coupling

The general current for the electromagnetic interaction between protons may take the form

$$J^\mu = e\bar{u}(p')[F_1\gamma^\mu + \frac{F_2}{2M}i\sigma^{\mu\nu}q_\nu]u(p), \quad (\text{D.1})$$

where $q_\nu \equiv p'_\nu - p_\nu$ is the momentum transfer during interaction, M is the proton mass, F_1 and F_2 are independent form factors and

$$\sigma^{\mu\nu} = \frac{i}{2}(\gamma^\mu\gamma^\nu - \gamma^\nu\gamma^\mu). \quad (\text{D.2})$$

The vertex function in the square bracket of (D.1) might be simplified in the way that the $\sigma_{\mu\nu}$ is not involved. We start by consider the term $i\sigma^{\mu\nu}q_\nu$, that is

$$\begin{aligned} \bar{u}i\sigma^{\mu\nu}q_\nu u &= \bar{u}i\sigma^{\mu\nu}p'_\nu u - \bar{u}i\sigma^{\mu\nu}p_\nu u \\ &= -\frac{1}{2}\bar{u}(\gamma^\mu\gamma^\nu - \gamma^\nu\gamma^\mu)p'_\nu + \frac{1}{2}\bar{u}(\gamma^\mu\gamma^\nu - \gamma^\nu\gamma^\mu)p_\nu u \\ &= \bar{u}(\gamma^\nu\gamma^\mu - g^{\mu\nu})p'_\nu u + \bar{u}(\gamma^\mu\gamma^\nu - g^{\mu\nu})p_\nu u \\ &= (M\bar{u}\gamma^\mu u - \bar{u}p'^\mu u) + (M\bar{u}\gamma^\mu u - \bar{u}p^\mu u) \\ &= 2M\bar{u}\gamma^\mu u - \bar{u}(p'^\mu + p^\mu)u \end{aligned} \quad (\text{D.3})$$

or

$$\bar{u}(p')\gamma^\mu u(p) = \frac{1}{2M}\bar{u}(p')[(p' + p)^\mu + i\sigma^{\mu\nu}(p' - p)_\nu]u(p). \quad (\text{D.4})$$

(D.4) is also known as *Gordon decomposition*.

In the above derivation, we have used the following relations for $u(p)$ and $\bar{u}(p')$

$$(\gamma^\mu p_\mu - M)u(p) = 0, \quad (\text{D.5})$$

$$\bar{u}(p')(\gamma^\mu p'_\mu - M) = 0. \quad (\text{D.6})$$

Thus, (D.1) becomes

$$\begin{aligned} J^\mu &= e\bar{u}(p')[F_1\gamma^\mu + \frac{F_2}{2M}i\sigma^{\mu\nu}q_\nu]u(p) \\ &= e\bar{u}(p')[F_1\gamma^\mu + \frac{F_2}{2M}2m\gamma^\mu - (p'^\mu + p^\mu)]u(p) \\ &= e\bar{u}(p')[(F_1 + F_2)\gamma^\mu - \frac{F_2}{2M}(p'^\mu + p^\mu)]u(p). \end{aligned} \quad (\text{D.7})$$

Hence, one may express the vertex function in the form

$$F_1\gamma^\mu + \frac{F_2}{2M}i\sigma^{\mu\nu}(p'_\nu - p_\nu) = (F_1 + F_2)\gamma^\mu - \frac{F_2}{2M}(p'^\mu + p^\mu). \quad (\text{D.8})$$

D.2 Vertex Function for $NN\rho$ Coupling

The Lagrangian for the $NN\rho$ coupling takes the form

$$\mathcal{L}_{pp\rho} = g_{pp\rho}\bar{\psi}\gamma_\mu\psi\phi_\rho^\mu + \frac{g'_{pp\rho}}{4M}\bar{\psi}\sigma_{\mu\nu}\psi(\partial^\mu\phi_\rho^\nu - \partial^\nu\phi_\rho^\mu), \quad (\text{D.9})$$

where $\sigma_{\mu\nu}$ is defined by

$$\sigma_{\mu\nu} = \frac{i}{2}(\gamma_\mu\gamma_\nu - \gamma_\nu\gamma_\mu). \quad (\text{D.10})$$

The vertex function can be obtained from the Lagrangian by eliminating all the fields. Since there is no operator acting on $\bar{\psi}$ and ψ , we can eliminate $\bar{\psi}$ and ψ

immediately and we get

$$\begin{aligned} g_{pp\rho}\gamma_\mu\phi_\rho^\mu + \frac{g'_{pp\rho}}{4M}\sigma_{\mu\nu}(\partial^\mu\phi_\rho^\nu - \partial^\nu\phi_\rho^\mu) &= g_{pp\rho}\gamma_\nu\phi_\rho^\nu + \frac{g'_{pp\rho}}{2M}\sigma_{\mu\nu}\partial^\mu\phi_\rho^\nu \\ &= g_{pp\rho}\gamma_\nu\phi_\rho^\nu + \frac{g'_{pp\rho}}{2M}\sigma_{\mu\nu}(-iq^\mu)\phi_\rho^\nu, \end{aligned}$$

where we have used the relation

$$\begin{aligned} \sigma_{\mu\nu}\partial^\nu\phi_\rho^\mu &= \sigma_{\nu\mu}\partial^\mu\phi_\rho^\nu \\ &= -\sigma_{\mu\nu}\partial^\mu\phi_\rho^\nu. \end{aligned} \quad (\text{D.11})$$

Thus, after eliminate ϕ_ρ^ν , the vertex function for the $NN\rho$ coupling becomes

$$g_{pp\rho}\gamma_\nu - \frac{g'_{pp\rho}}{2M}i\sigma_{\mu\nu}q^\mu. \quad (\text{D.12})$$

In the same way as for the $NN\gamma$ coupling, we derive

$$i\sigma_{\mu\nu}q^\mu = (p'_\nu + p_\nu) - 2M\gamma_\nu. \quad (\text{D.13})$$

Thus, from (D.12) and (D.13), the vertex function for the $NN\rho$ coupling is expressed as

$$\begin{aligned} g_{pp\rho}\gamma_\nu - \frac{g'_{pp\rho}}{2M}i\sigma_{\mu\nu}q^\mu &= (g_{pp\rho} + g'_{pp\rho})\gamma_\nu - \frac{g'_{pp\rho}}{2M}(p'_\nu + p_\nu) \\ &= g_{pp\rho}[(1 + f_{pp\rho})\gamma_\nu - \frac{f_{pp\rho}}{2M}(p'_\nu + p_\nu)], \end{aligned} \quad (\text{D.14})$$

where $f_{pp\rho} \equiv g_{pp\rho}/g'_{pp\rho}$.

D.3 Vertex Function for NNf_2 Coupling

The Lagrangian for the NNf_2 coupling takes the form

$$\begin{aligned} \mathcal{L}_{ppf_2} &= i\frac{1}{2M}g_{ppf_2}(\bar{\psi}\gamma^\mu\partial^\nu\psi - \partial^\nu\bar{\psi}\gamma^\mu\psi)\phi_{f_2\mu\nu} + \frac{1}{2M^2}g'_{ppf_2}(\bar{\psi}\partial^\mu\partial^\nu\psi - \\ &\quad \partial^\mu\bar{\psi}\partial^\nu\psi - \partial^\nu\bar{\psi}\partial^\mu\psi + \partial^\mu\partial^\nu\bar{\psi}\psi)\phi_{f_2\mu\nu}. \end{aligned} \quad (\text{D.15})$$

Considering $\partial^\mu \psi(p) = -ip^\mu \psi(p)$ and $\partial^\mu \bar{\psi}(p') = ip^\mu \bar{\psi}(p')$, the vertex function for the NNf_2 coupling is derived as follows:

$$\begin{aligned}
 \Gamma(p, p') &= i \frac{1}{2M} g_{ppf_2} [\gamma^\mu (-ip^\nu) - (ip'^\nu) \gamma^\mu] + \frac{1}{2M^2} g'_{ppf_2} [(-ip^\mu)(-ip^\nu) \\
 &\quad - (ip'^\mu)(-ip^\nu) - (ip'^\nu)(-ip^\mu) + (ip'^\mu)(ip'^\nu)] \\
 &= \frac{1}{2M} g_{ppf_2} [\gamma^\mu (p^\nu + p'^\nu)] - \frac{1}{2M^2} g'_{ppf_2} [p^\mu p^\nu + p'^\mu p^\nu \\
 &\quad + p^\mu p'^\nu + p'^\mu p'^\nu] \\
 &= \frac{g_{ppf_2}}{2M} [\gamma^\mu (p^\nu + p'^\nu) - \frac{f_{ppf_2}}{M} (p^\mu p^\nu + p'^\mu p^\nu \\
 &\quad + p^\mu p'^\nu + p'^\mu p'^\nu)], \tag{D.16}
 \end{aligned}$$

where $f_{ppf_2} \equiv g'_{ppf_2}/g_{ppf_2}$.

Biography

Mr. Kem Pumsa-ard was born on July 22nd, 1975 in Bangkok. He has received the Development and Promotion of Science and Technology Talents Project (DPST) scholarship from the Institute for the Promotion of Teaching Science and Technology (IPST) since 1991 while he was in high school in Bangkok. He graduated from Mahidol University, with a B.Sc. Degree in Physics in 1998. After that he joined the School of Physics, Institute of Science, Suranaree University of Technology for a Master's Degree.